14 April 1941

NRL Report No. H-1723

NAVY DEPARTMENT

FR-123

Report

on

A Photoelastic Analysis of the Stresses in Fatigue Test Specimens

NAVAL RESEARCH LABORATORY
ANACOSTIA STATION
WASHINGTON, D. C.

Number of Pages: Text - 8 Tables - 2 Plates - 24

Authorization: BuC&R Ltr. P8/Eng. Foundation (DY1) of 23 January 1940.

Date of Test: 1 October 1940 to 1 April 1941

Prepared by: J. S. Brock, Contract Employee.

H. B. Maris, Associate Physicist.

Reviewed by: E.O.Hulburt, Principal Physicist, Supt. of Physical Optics Division.

Approved by: H. G. Bowen, Rear Admiral USN, Director.

Distribution: BuShips (7)

gfw

TABLE OF CONTENTS

APPENDICES

AUTHORIZATION

1. This investigation was authorized by Bureau of Construction and Repair letter P8/Eng. Foundation (DY1) of January 23, 1940.

PURPOSE

2. The purpose of this investigation was to make a photoelastic analysis of the stresses in fatigue test specimens subjected to static loads. No attempt has been made to study the fatigue elements of the problem.

MODELS AND LOADING DEVICE

3. Table 1 gives a compact description of the celluloid models tested in this investigation. Column 1 identifies the model by letter and also gives the radius of the fillet which connects the throat of each specimen to the head (i.e.) to the portion having maximum width. The thickness of the individual models is recorded in Column 2 and the head width and throat width are given in Column 3 and Column 4 respectively. Column 5 gives further identifying remarks. Welded specimens marked A and E are plain one-piece plates. It would be difficult to make a butt weld, using plastics, of sufficient strength to take the loads required to determine the stress distribution. The effect of a plastic weld on the stress pattern of a plastic model will tell us nothing of the effects of a steel weld on a steel model. In each case the influence of the weld would be a measure of its interference with the normal elastic properties of the model, and since the characteristics of the two welds are different, their elastic effects would not be comparable.

4. Tee welds were applied to both sides of specimens marked F. Riveted specimens marked B, C, D, were made with both celluloid and Plexiglas straps; the reason for this will appear later. The diameter of the rivets for Models B and C was 5/16 inch, while the diameter of the rivets for Model D was 13/32 inch. Brass bolts were used for rivets in all cases. The rivet holes were countersunk on both sides of the joint, in the case of the celluloid straps. Small conical washers were pressed out of solder to fit in the countersunk holes in order to simulate the stresses due to a real rivet. In addition to the models of actual test specimens, a plain model was constructed similar to Model B. Rivet holes were drilled and plugged with brass but no straps were applied.

5. Plate 24 is a photograph of a model in the loading device which is a Duralumin framework designed to exert a pure tension on the model.

RELATED EXPERIMENTS

6. The problem of the determination of the stress distribution due to the action of a rivet has been treated mathematically by Knight(1), and Frocht and Hill(2) have attacked the problem using the photoelastic

method of stress analysis and strain gage measurements. Coker[3] has also investigated the stress distribution in a plate due to a load on a rivet. These papers deal with the problem of stress analysis in a riveted joint in its very simplest form, that is simple joints with one pin or rivet, and give no idea of the stress concentrations to expect in a complicated joint.

7. The actual fatigue strength of riveted and welded joints has been studied experimentally by W.M.Wilson and others [4]. It must be remembered that the stress patterns presented in this report are for static loads within the elastic limit and that the stress distribution in a riveted or welded joint would probably change considerably with plastic deformation. The stress concentration factors represent upper limits. One would expect that the stress concentrations in a steel specimen causing failure under fatigue would be somewhat less than those shown here for static loads. Tests on celluloid cannot be used as a basis of an estimate of the reduction in concentration factors due to plastic yielding in steel.

OPTICAL ARRANGEMENT

8. The optical arrangement used in this investigation, arranged as shown by the schematic diagram on Plate 22, consisted of a mercury arc source S, polarizer P, compensator C, lens combination L, model M, quarter wave plate Q, analyzer A, objective O, ground glass G or photographic plate. Filters and stops are not shown on this diagram. Isoclinics were traced with the compensator and quarter wave plate removed, and isochromatics were traced with the compensator in place, but with the quarter wave plate removed. Photographs were made of the strap joint with the compensator C adjusted so as to act as a quarter wave plate and with the quarter wave plate Q also in place. This arrangement caused the light passing the model to be circularly polarized so that the isoclinic or lines of equal inclination of the principal stress would not show up in the pattern to be photographed. An arrangement of this nature is necessary when the stress distribution is so complicated that the isoclinics show up for all angular positions of the polariscope.

BRIEF OF RESULTS

9. The stress patterns for Models A and E are for plane filleted strips. Local stress concentrations would be found in the immediate vicinity of the steel weld but the magnitude and distribution of these would depend on the skill of the welder and could not be duplicated in celluloid. Model A 1.7R shows a stress concentration of about 30% more than the applied stress at the base of the fillet. Models A and E 4.8R show very similar patterns with stress concentrations of about 13% at the base of the fillet. Models F 1.6R and F 2.4R with a horizontal tee welds show stress concentration of about 25% more than the applied stress, while Model F 4.8R shows only a 15% increase in stress concentration. In addition to the effect of the fillets a local tensile cross stress of about 20% of the applied stress arises due to the presence of the tee welds on these specimens. Riveted joint specimens B 1.7R and

B 4.8R show stress concentrations of approximately 30% and 15% respectively at the fillets. Models C 4.8R and D 1.8R show an increase in stress of about 15% due to the presence of the fillets. Stress patterns for the plain model indicate that the important points of stress concentration in the riveted specimens are around the rivet holes where the stress is approximately 3 times the value of the applied stress. Table 2 shows in compact form the maximum concentration factors for all models tested.

DESCRIPTION OF INDIVIDUAL PLATES

10. Plate 1 shows the isoclinic pattern for Model A 1.7R in quadrants 3 and 4. These lines were traced for both ends of the model and the pattern shown is a composite or average of the two originals. The zero isoclinic lines show the extent of the disturbance from uniform stress condition produced by the discountinuity of the filleted structure. The dotted lines thus bound the area over which the stress is uniform. The isostatic or stress flow lines are shown in quadrants 1 and 2. These lines of principal stress, which are derived from the isoclinic pattern, show the direction in which the P and Q stresses act.

11. Plate 2 shows the isochromatic pattern for Model A 1.7R in quadrants 3 and 4. On any isochromatic line the stress difference P-Q remains constant in magnitude. The isochromatic marked 1.0 represents the applied stress, and the values of P-Q over the other isochromatics are relative to the value of the applied tensile stress. It is only necessary to multiply each of these values by the applied stress in order to determine the stress difference in a steel plate of the same relative dimensions if the elastic limit is not exceeded. Quadrants 1 and 2 show results of stress exploration along the vertical center line and along the fillet contour. The P and Q stresses were separated by the usual method of numerical integration(3). Curve P shows that the vertical tensile stress remains near unity as one proceeds along the vertical center line until the fillet is reached, where it decreases gradually to 0.68 of the applied stress. This latter value would probably be somewhat lower if the load were applied uniformly across the end of the model. Curve P-Q shows the variation of the stress difference along the vertical center line. The Q curve is obtained by subtracting the stress difference P-Q from the integrated values of the P stress. The cross stress Q is zero in the straight portion of the model. It then increases as a tension to a maximum value of 0.2T about the middle of the fillet where it decreases to zero near the end of the fillet and finally becomes a compressive stress, the maximum value of which is 0.15T, where T is the average applied stress. The remaining curve shows the variation of the contour stress around the fillet. The maximum value of about 1.3 T occurs just beyond the joint of the straight portion. This is the point of highest stress on the model and the maximum value of the stress concentration factor is 1.3, where this factor is defined as the ratio of the maximum stress to the applied stress. Plates 2, 4 and 6 indicate that an increase in the length of the model either in the throat or in the shoulder would not appreciably change the pattern

of stress distribution at the fillet. This applies to Models A, E and F, but it does not apply to Models B, C, and D.

12. Plate 3 shows the isostatic and isoclinic patterns in quadrants 1-2 and 3-4 respectively for Model A 4.8R. As before, the dotted lines show the portion of the model which is under pure tension. The splitting of the zero isoclinic line near the lower part of the pattern is probably caused by the presence of the first two loading bolts marked by x's on Plate 24.

13. Plate 4 shows curves of stress distribution and the isochromatic pattern in quadrants 1-2 and 3-4 respectively for Model A 4.8R. The curve Q indicates that the maximum value of the tensile cross stress is about 0.2 T. This maximum occurs about half-way across the fillet. The Q stress then decreases, but does not become a compressive stress due to the fact that the loading plate prevents an exploration of the stress beyond the fillet. This was not true for the fillet of small radius. The P stress decreases from unity to 0.7 T as one proceeds upward along the vertical center line.

14. Plate 5 shows the isostatic and isoclinic patterns for Model E 4.8R in quadrants 1-2 and 3-4 respectively. The asymmetrical nature of the isoclinics indicates the presence of a bending of flexure moment on the model. This moment is due to one side of the model assuming the load before the other and is caused by imperfections in shop work. A part of the non-symmetry might be attributed to initial stress in the model material. The asymmetrical condition is also evident from the lines of principal stress.

15. Plate 6 shows the curves of stress distribution and the isochromatic pattern for Model E 4.8R in quadrants 1-2 and 3-4 respectively. Due to the non-symmetrical character of the isoclinic lines, integrations will not be as accurate as usual. However, the Q curve shows that the maximum cross stress is approximately 0.17 T. P-Q, the stress difference decreases to 0.65 T and P decreases from the value of the applied stress in the straight portion to 0.65 at the upper boundary. The maximum stress concentration factor occurs near the beginning of the fillet and is about 1.13.

16. Plate 7 shows isoclinic and isostatic patterns in quadrants 1-2 and 3-4 respectively for Model F 1.6R which represents a tee welded joint. The dotted lines bound the area of the specimen which is in a uniform stress condition. Neither P nor Q vary an appreciable amount in this section, thus the lines of principal stress are straight between the dotted lines. Near the tee weld, isoclinics of parameter other than zero show up and indicate a variation in the stress distribution in the vicinity of the weld.

17. Plate 8 shows stress exploration curves and the isochromatic map for Model F 1.6R in quadrants 1-2 and 3-4 respectively. The P-Q curve shows the variation in the principal stress difference along the vertical center line. The value of P-Q is about 0.8T near the weld and

increases slightly only to decrease to about 0.7T in passing the fillet. It finally increases to a little more than 0.8T near the upper boundary of the specimen. Q is about 0.2T along the straight portion of the model; it then decreases and finally becomes a compressive stress which reaches a maximum of about 0.15 T. P decreases from the value of the applied stress to about 0.65T at the upper boundary. The contour stress is a maximum of about 1.25T near the beginning of the fillet, thus the maximum stress concentration factor is 1.25.

18. Plate 9 shows the isoclinic and isostatic patterns for Model F 2.4R in quadrants 1-2 and 3-4 respectively. They are very similar to the corresponding patterns for Model F 1.6R.

19. The stress exploration curves and isochromatic pattern are shown on Plate 10 for specimen F 2.4R. Curve Q shows that the magnitude of the cross stress is about 0.2T near the tee weld and is zero near the end of the fillet above which there is a small compressive cross stress. P decreases from 1.0T to about 0.7T along the vertical center line. The contour stress shows a maximum of approximately 1.25T near the beginning of the fillet and then gradually falls off as one goes around the fillet radius.

20. Plate 11 shows the isoclinic and stress flow maps for Model F 4.8R. Except for the isoclinics having parameters of $\pm$ 2° near the tee weld, these patterns are very much like the corresponding ones for Model A 4.8R. It is of interest to note that the isoclinics, if extended, would meet the edge of the specimen where this edge is inclined with respect to the vertical line an amount equal to the parameter of the isoclinic. This is equivalent to the statement that the stress along a free boundary is everywhere parallel to it.

21. Plate 12 shows the curves of stress distribution and the isochromatic pattern for Model F 4.8R. Curve P shows that the longitudinal tensile stress decreases from the value of the applied stress to 0.78T along the vertical center line. The stress difference first increases from about 0.8T to 0.85T, then decreases to approximately 0.7T, but finally increases to about 0.8T near the upper boundary. Curve Q shows the variation of the cross stress along the vertical center line. The maximum value of this tensile cross stress is about 0.2 times the value of the applied stress and the minimum value is close to zero at the upper boundary. The maximum contour stress is 1.15 times the applied stress.

22. Plate 13 shows the isoclinic and isostatic patterns for Model B 1.7R, a riveted specimen with the shape of the double strap indicated. The isostatic lines are superimposed on the isoclinics. It was not feasible to make a composite pattern as was done for the models not having the riveted joint due to the non-symmetrical nature of the isoclinic pattern. This asymmetry in the stress direction is caused by the imperfections in fabrication and would also be present in steel specimens. The stress distribution will thus be complicated in all riveted specimens. A discussion of the stresses in the strap joint will appear later.

23. Plate 14 shows the isochromatic stress pattern for Model B 1.7R with a load of 450 pounds. This pattern is also non-symmetrical and indicates that the stress distribution is complex. High values of the stress difference are found at the fillets and also in the center of the model near the loading plates. The maximum stress concentration for this specimen is about 1.3 outside the strap joint. Integrated values of the P and Q stresses are not shown due to the fact that the process is inaccurate unless the stress patterns are symmetrical. Also it will be shown that the stress concentrations outside the joint are not important except near the fillets as compared to those under the joint near the rivets.

24. Plate 15 shows the isoclinic and isostatic patterns for Model B 4.8R. Again the asymmetry of the patterns is very pronounced. Some of this asymmetry is due to initial stress, but most of it is introduced by imperfect machining and assembling of the model. Obviously, it is unavoidable in a complicated joint.

25. Plate 16 shows the isochromatic map for Model B 4.8R under a load of 450 pounds with a celluloid strap and taut rivets. The maximum stress concentration factor outside the strap joint is about 1.15.

26. Plate 17 shows the isoclinic and isostatic maps for Model C 4.8R. The isoclinic pattern, which is not supposed to change with the load, did show variation with load changes. This can only happen when there is an appreciable initial stress if the elastic limit is not exceeded. The applied stress was 555 pounds per square inch, which is well below the elastic limit for celluloid (2,000 pounds per square inch).

26. Plate 18 is a map of the isochromatic lines for Model C 4.8R under a load of 450 pounds and with rivets taut. The maximum stress concentration factor for this specimen occurs at the fillets and is about 1.15 T in magnitude. It will be understood that this factor is not the maximum stress under the joint. The small difference in the straps for Models B and C does not have any appreciable effect on the maximum stress concentration factors.

28. The isoclinic map and stress flow lines are shown on Plate 19 for Model D 1.8R under a load of 500 pounds. The rivets were taut. Both the isoclinic and isostatic maps show the asymmetry of the stress distribution.

29. Plate 20 shows the isochromatic pattern for Model D 1.8R loaded to 440 pounds and with taut rivets. Low values of P-Q show up between the protrusions of the strap. This indicates a comparatively high tensile Q stress. It is due to the prevention of the natural lateral contraction of the external plate by the rigidity of the straps. The stress difference in a steel specimen would be slightly less than that in the celluloid model due to the fact that Poisson's ratio is less for steel. This effect would not be important. At the fillets, this model showed a stress concentration of about 1.15.

30. Plate 21 shows stress patterns for a plain one piece model without a strap. These patterns are presented to give a measure of the stress condition to expect under the strap. The isoclinic lines are very symmetrical as compared to the corresponding patterns for Models B, C, and D. Only zero isoclinics are drawn amongst the plugged holes due to the small space available. There would be isoclinic lines of parameter other than zero as the stress directions change rapidly in the vicinity of a discontinuity. The isochromatic map shows that the stress concentration is about 1.25 at the fillets and approximately 3.0 on either side of the plugged holes. The latter figure is probably the stress concentration to expect under the strap of a riveted joint. Thus the relatively small stress concentration factors found at the fillets are not important as compared to the much larger concentration factor near the rivets.

31. Four photographs of Model B 1.7R under different conditions are shown on Plate 23. These photographs of the double strap joint taken with circularly polarized light show a summation of the double refraction which takes place in each of the individual layers of the stressed material; that is, they show the total double refraction due to stress in the plate and to the stress in the double straps. Photograph A shows the stress pattern in the celluloid strap joint with no tensional load applied. The rivets were drawn taut on one side of the horizontal center line, but were loose on the other side. The resulting pattern shows the effect of the tensile stress of the rivets. Second order green lines are marked, while first and third order lines are not labeled due to lack of space. Usually the black dots represent neutral points, i.e., where P-Q=0. The stress gradient is very high in the vicinity of the rivets as is shown by the crowding of the stress lines. Photograph B shows the same model under the same conditions, except that a load of 1,000 pounds was applied to the specimen. The second order green lines are labeled as on Photograph A. In the external plate, the stress lines at the fillets are more prominent on the end of the specimen in which the rivets were not taut. Therefore, taut rivets reduce the maximum stress concentration factors in the external plate because the frictional grip of the strap distributes the applied load more uniformly than would be the case with loose rivets.

32. Photograph C shows the stress pattern for the same model under no load but with a Plexiglas strap. Plexiglas was used because it has a very small negative stress optical coefficient as compared to celluloid, so that the double refraction in the strap is small as compared to that in the plate. The negative stress optical coefficient means that the stress effects in the Plexiglas straps subtract from the stress effect in the celluloid plate. The rivets were taut on one side of the horizontal center line as is shown by the round appearance of the hexagonal rivet heads. This is due to circular stress lines just under the rivet heads. No second order lines show up; therefore, most of the stress lines in Photograph A are due to stresses in the countersunk strap which arise from rivet tension. Photograph D shows the same model under a load of 1,000 pounds. Still no second order lines are visible. Stress lines show up at the fillets of the external plate with more prominence on the side of the specimen in which the rivets were not drawn taut showing again that taut rivets reduce

stress concentrations in the external plate.. Photographs of the straps of the other specimens would show in general the same condition and are therefore not included.

MISCELLANEOUS TESTS AND DISCUSSION

33. The loading device was modified so that models could be examined under compressive as well as tensile stresses. Patterns, not shown in the report, were traced and they indicate that the stress distribution in a specimen under compression is essentially the same as before. The maximum stress concentration factors were found to be approximately the same as for tensile loads.

34. Models B, C, and D were visually examined under various conditions of rivet tension. It was found that the stress distribution depends upon the tension in the individual rivet and also on the tightness of the bolts in the loading plate. Thus the stress distribution depends upon so many variables that patterns are asymmetrical and exact analysis is therefore difficult. A visual examination of the riveted models showed that the highest stress concentrations occurred at rivets marked X on Plate 24. These rivets assume the load in advance of the others and failures could be expected to start here.

References

1. "Action of a Rivet in a Plate of Finite Breadth" by R. C. Knight, Phil. Mag. Vol. 19, pp. 517-540 (1935).

2. "Stress-Concentration Factors Around a Central Circular Hole in a Plate Loaded Through Pin in the Hole" by M.M. Frocht and H.N.Hill, Journal of Applied Mechanics, Trans. A.S.M.E. Vol. 7, 1940, p. A-5.

3. Photoelasticity, by E.G.Coker and L.N.G.Filon, 1931, p. 525.

4. "Fatigue Tests of Riveted Joints", and "Fatigue Tests of Welded Joints in Structural Plates", by W. M. Wilson and others, Eng. Expt. Station Bull. Nos. 302 and 327, Univ. of Ill.

TABLE 1.

Model Description

Model Letter	Thickness t (in)	Width above fillet D (in)	Width below fillet d (in)	Identification Remarks
A 1.7R	.20	5.6	2.7	Butt weld
A 4.8R	.20	5.6	2.7	Specimens
B 1.7R	.20	6.4	4.5	Riveted joint
B 4.8R	.20	6.4	4.5	Specimens
C 4.8R	.20	6.4	4.5	Specimens
D 1.8R	.26	6.4	4.4	Specimens
E 4.8R	.25	5.6	2.7	Butt weld specimen
F 1.6R	.26	5.6	2.7	Tee weld
F 2.4R	.26	5.6	2.7	Specimens
F 4.8R	.25	5.6	2.7	Specimens
Plain model 4.8R	.20	6.4	4.5	Plugged hole plane model

TABLE 2

Maximum Stress Concentration Factors

Model letter and identification	Max. Stress Concentration Factor at Fillets	Max. Stress Concentration Factor under Strap Joint
A 1.7R Butt weld	1.30	-
A 4.8R Butt weld	1.13	-
B 1.7R Riveted specimen	1.30	>3
B 4.8R Riveted specimen	1.15	>3
C 4.8R Riveted specimen	1.15	>3
D 1.8R Riveted specimen	1.15	>3
E 4.8R Butt weld	1.13	-
F 1.6R Tee weld	1.25	-
F 2.4R Tee weld	1.25	-
F 4.8R Tee weld	1.15	-
Plain model	1.25	3.0

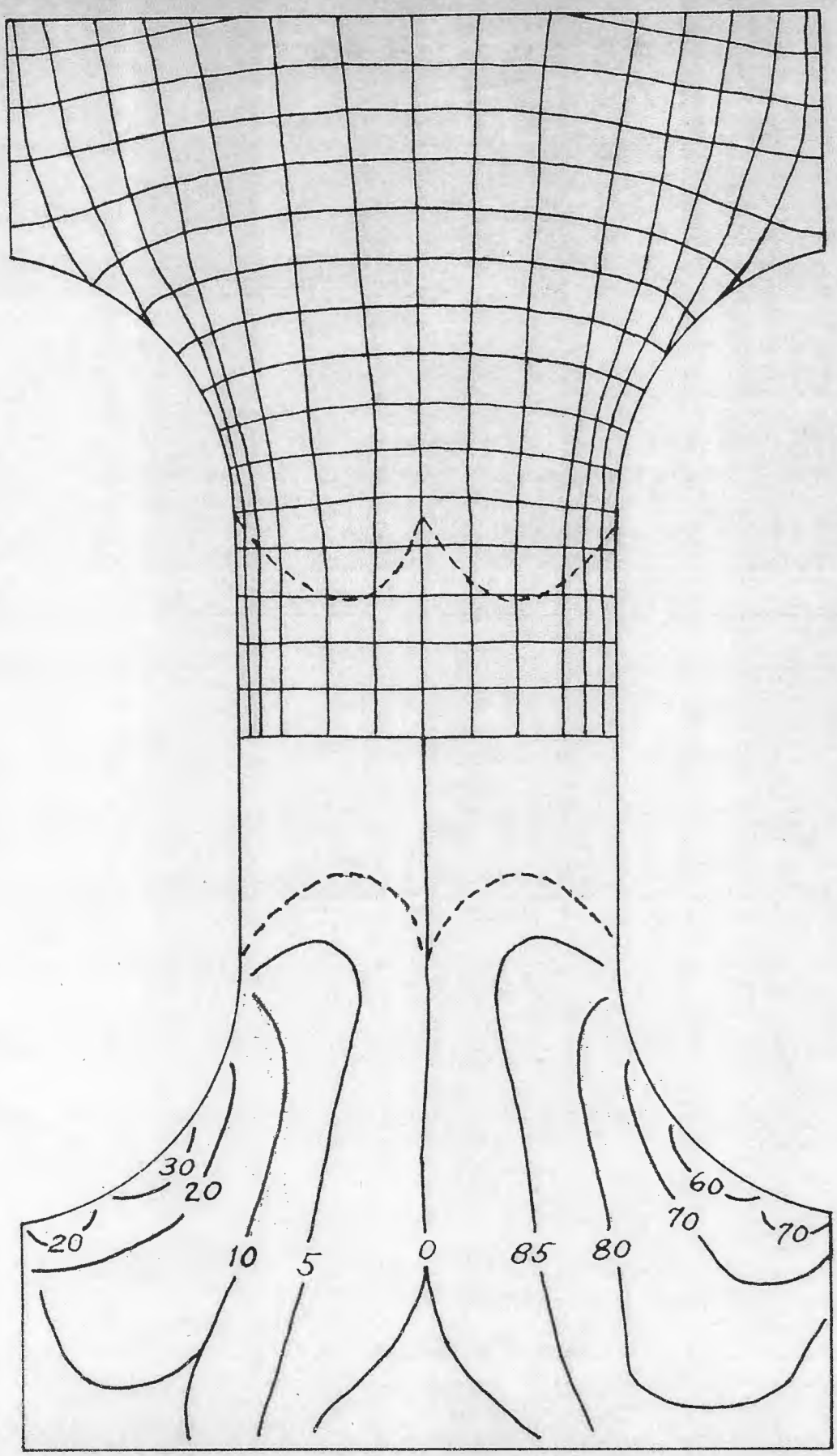

ISOSTATIC AND ISOCLINIC MAPS, MODEL A 1.7 R.

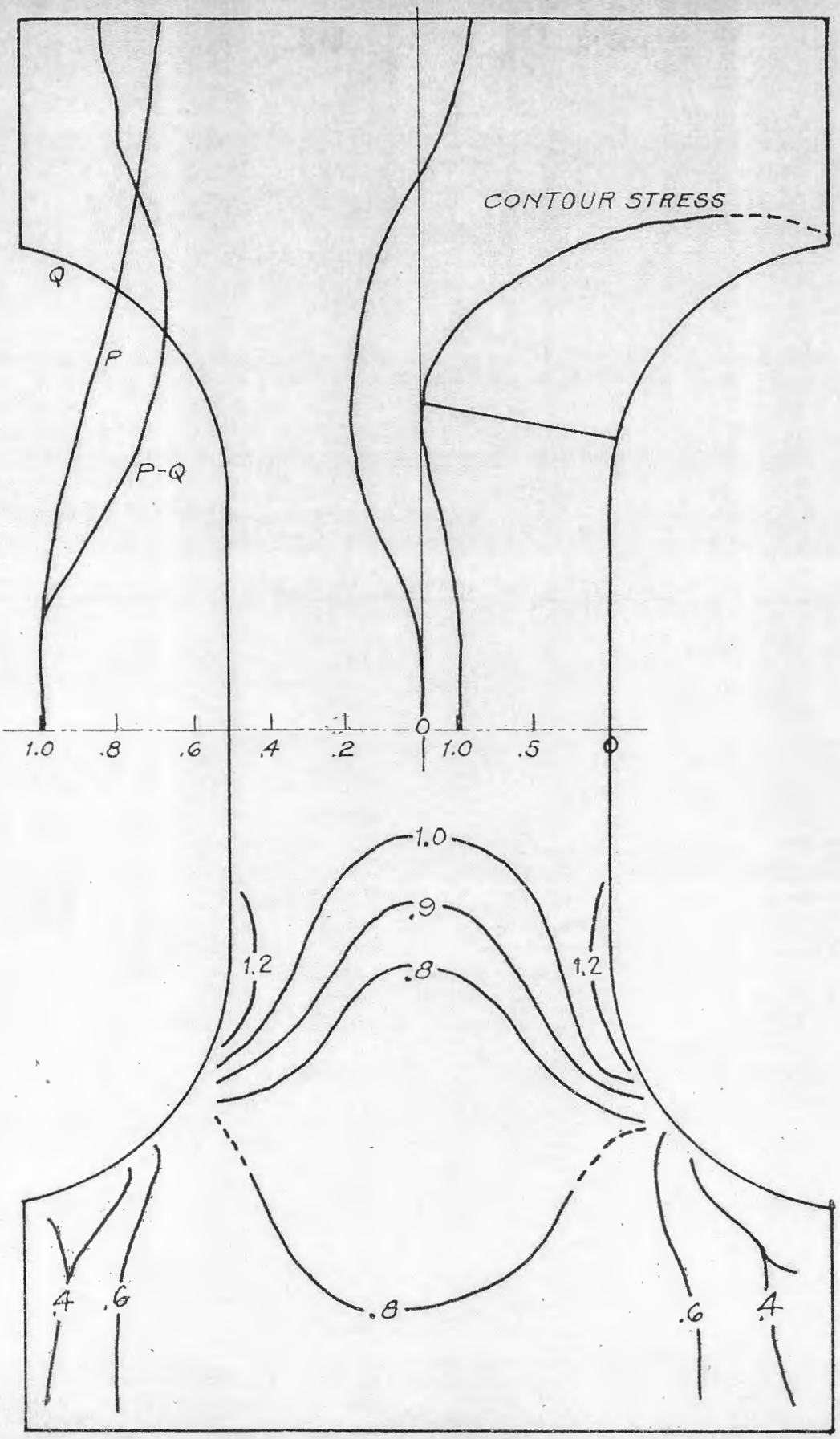

STRESS CURVES AND ISOCHROMATIC MAP, MODEL A 1.7 R.

PLATE 2

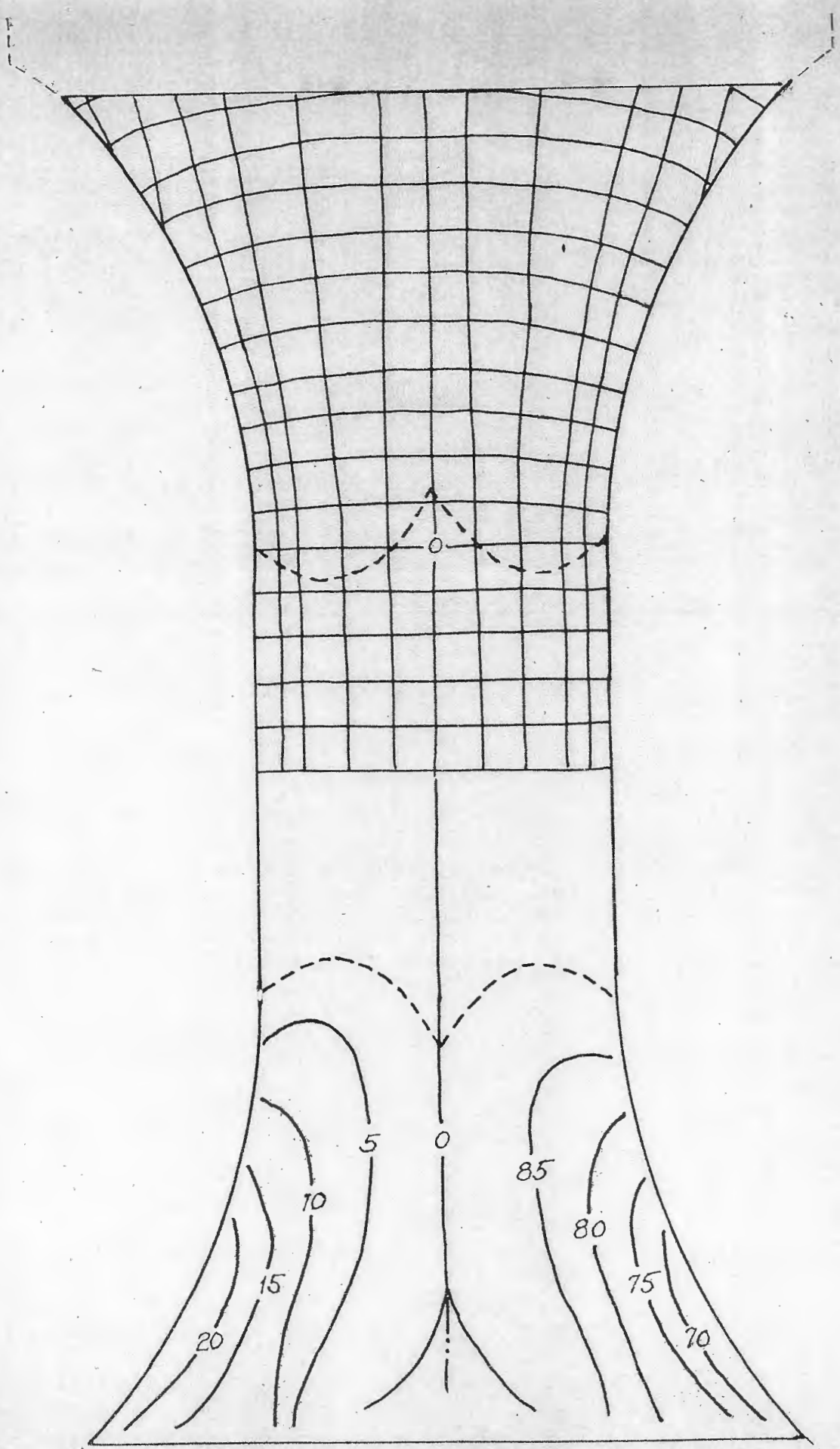

ISOSTATIC AND ISOCLINIC MAPS, MODEL A 4.8 R.

PLATE 3

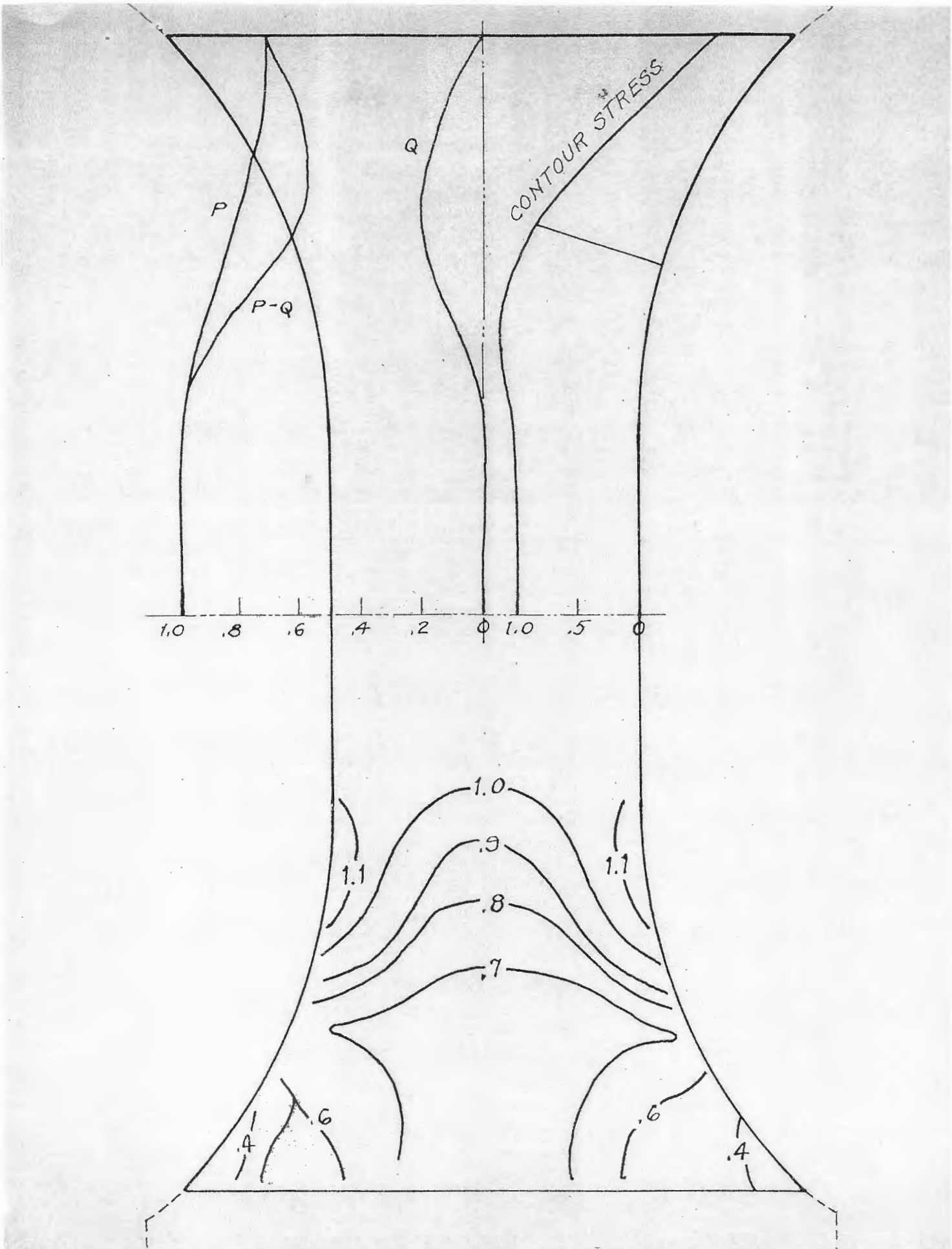

STRESS CURVES AND ISOCHROMATIC MAP, MODEL A 4.8 R.

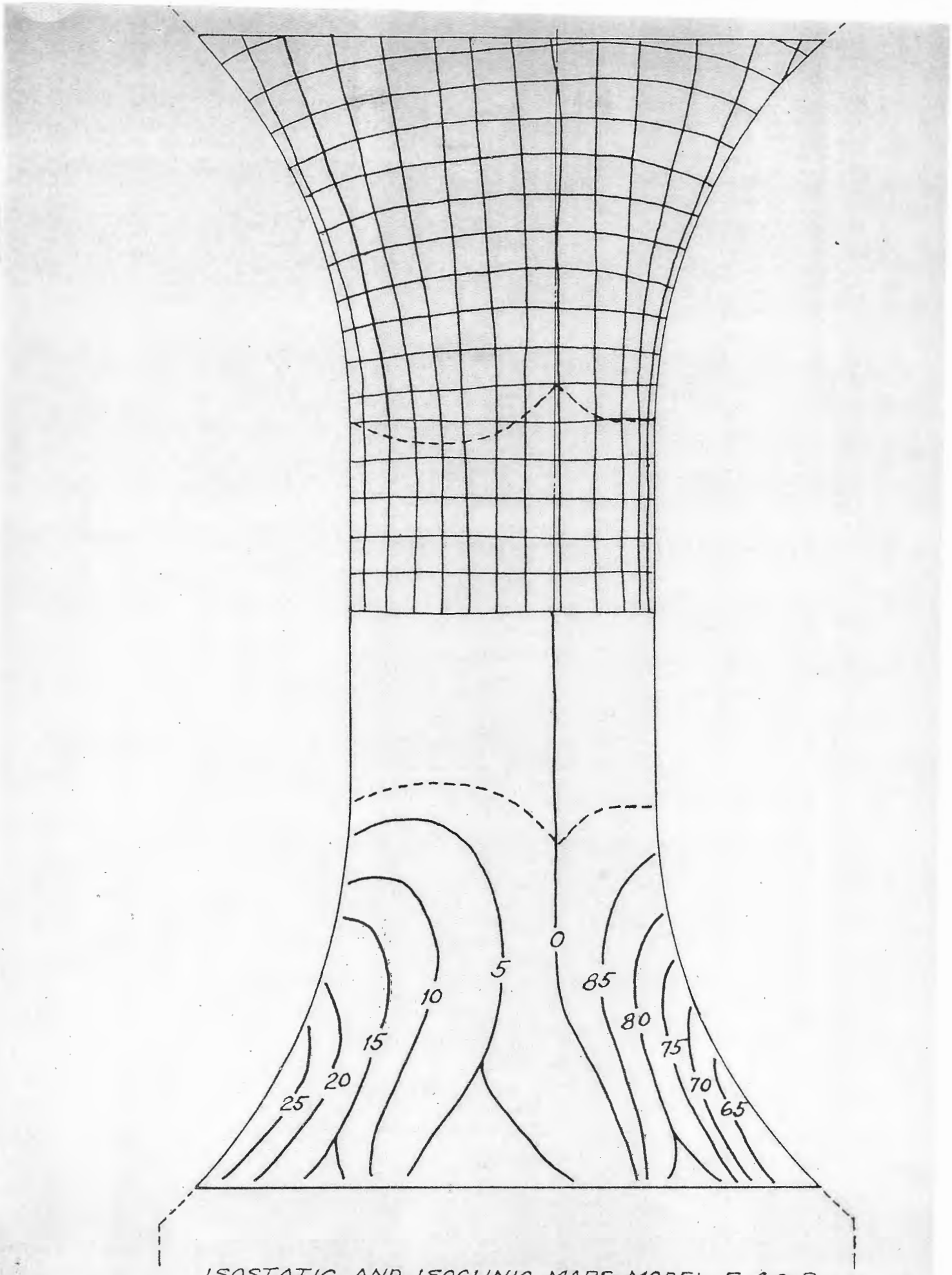

ISOSTATIC AND ISOCLINIC MAPS, MODEL E 4.8 R.

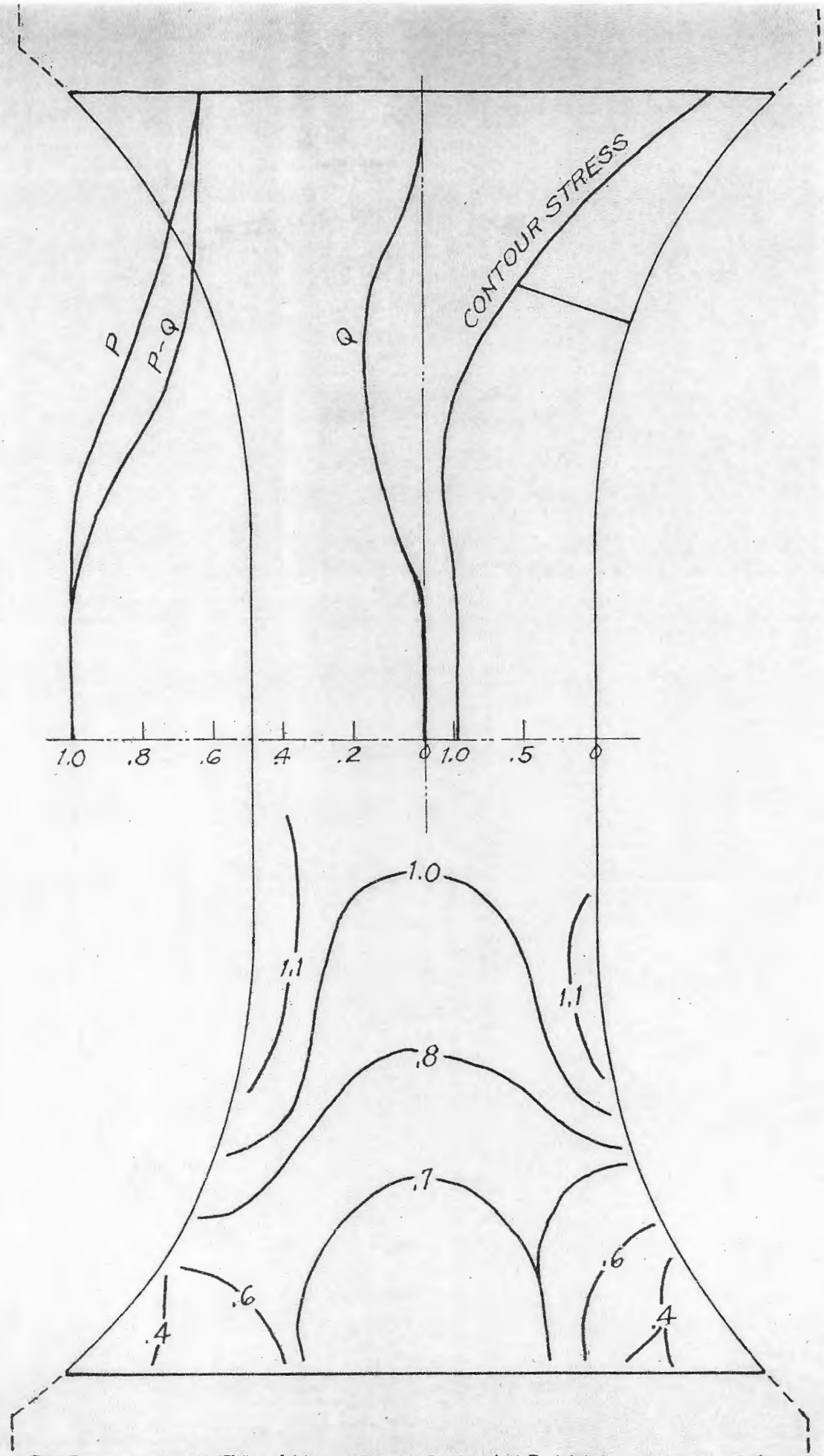

STRESS CURVES AND ISOCHROMATIC MAP, MODEL E 4.8 R.

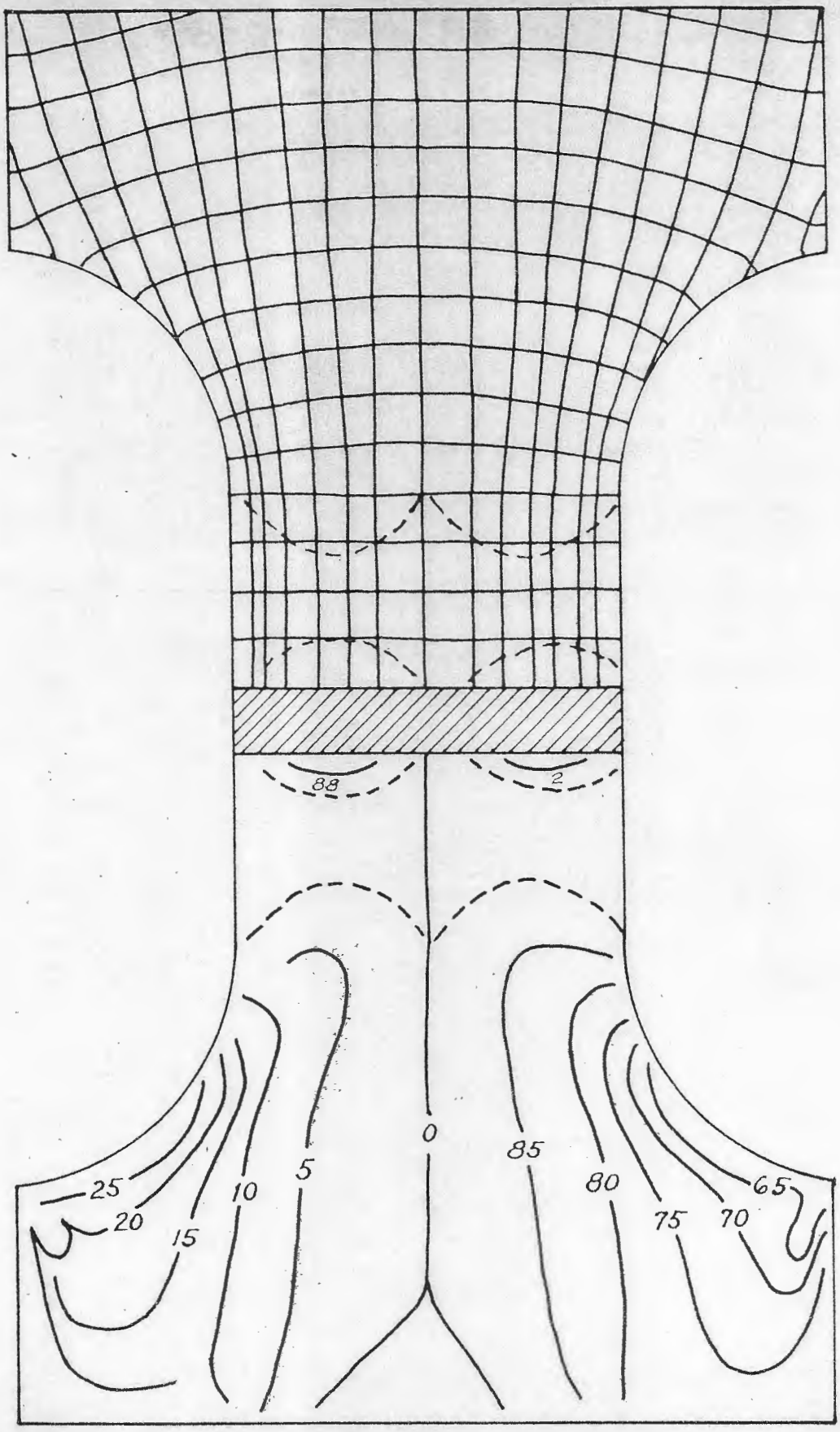

ISOSTATIC AND ISOCLINIC MAPS, MODEL F 1.6 R.

PLATE 7

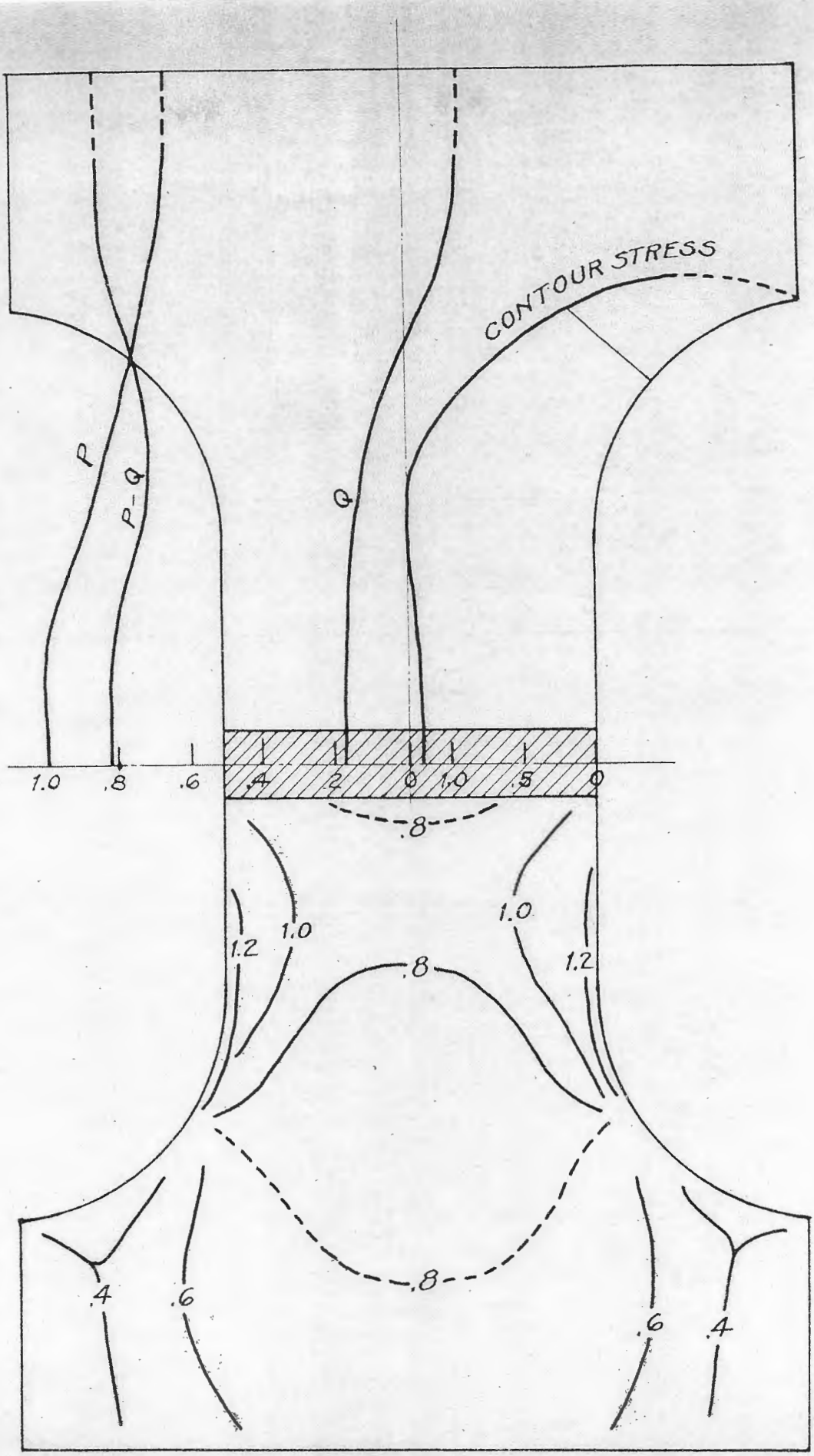

STRESS CURVES AND ISOCHROMATIC MAP, MODEL F 1.6 R.

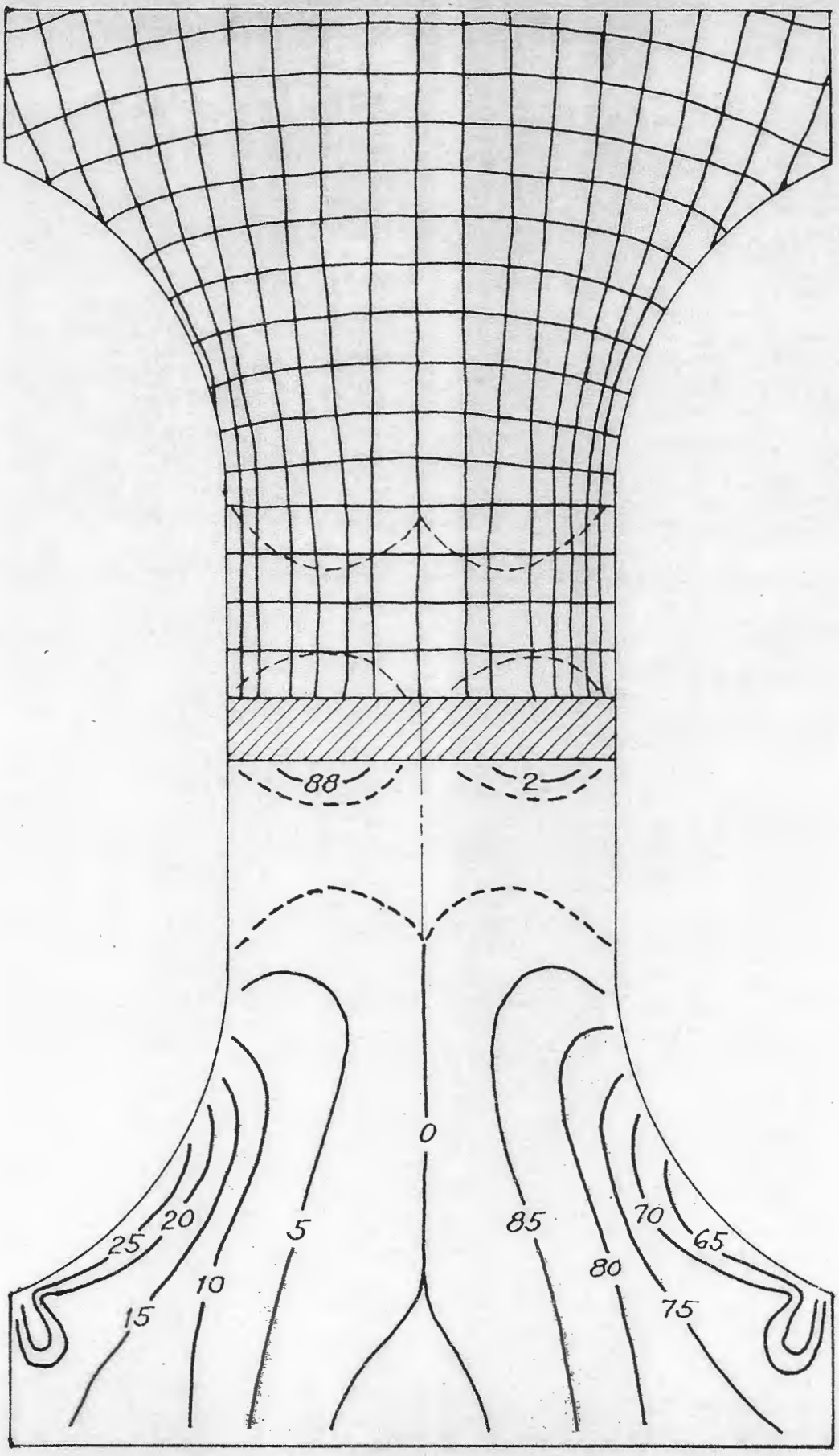

ISOSTATIC AND ISOCLINIC MAPS, MODEL F 2.4 R.

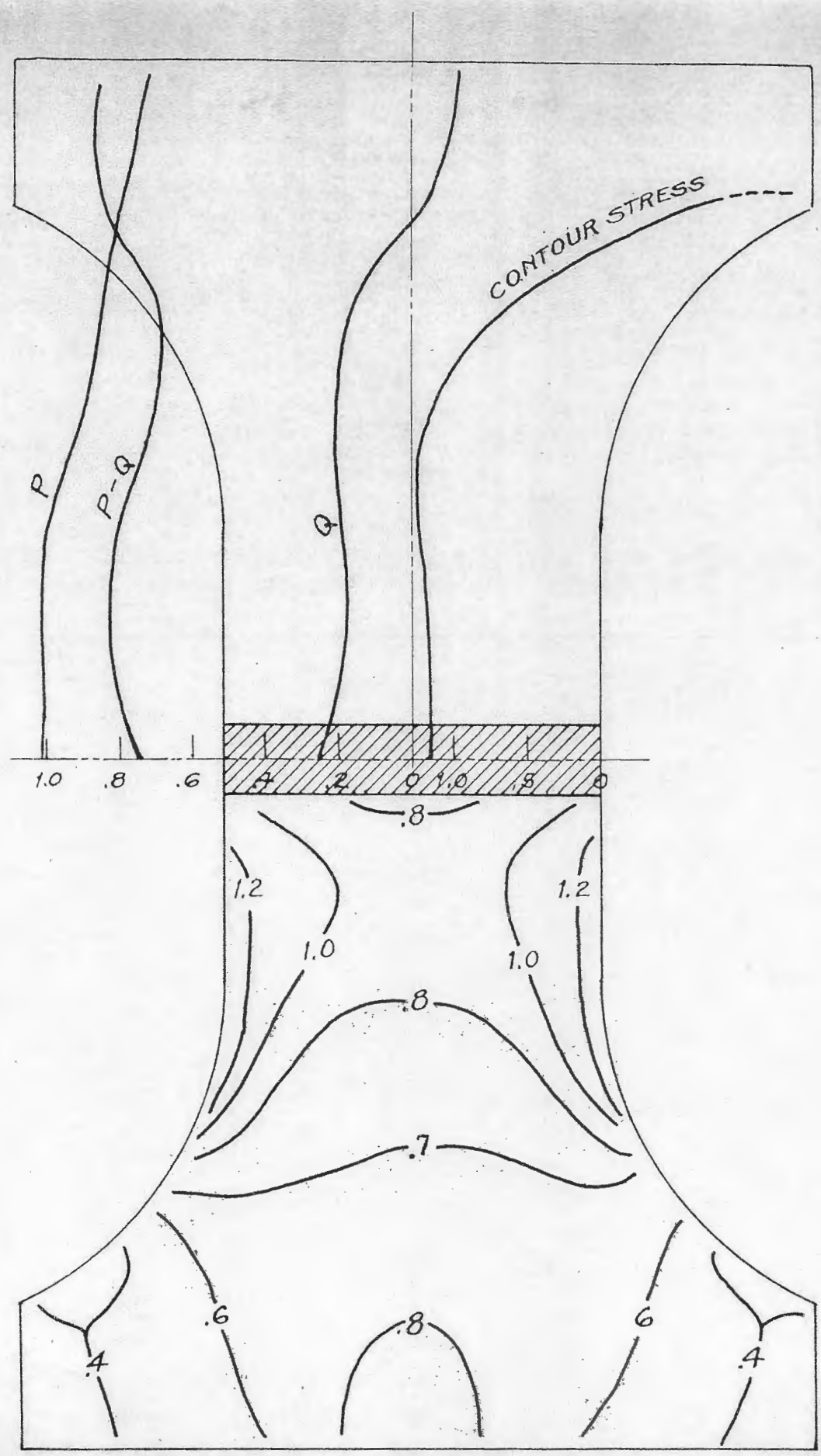

STRESS CURVES AND ISOCHROMATIC MAP, MODEL F 2.4 R.

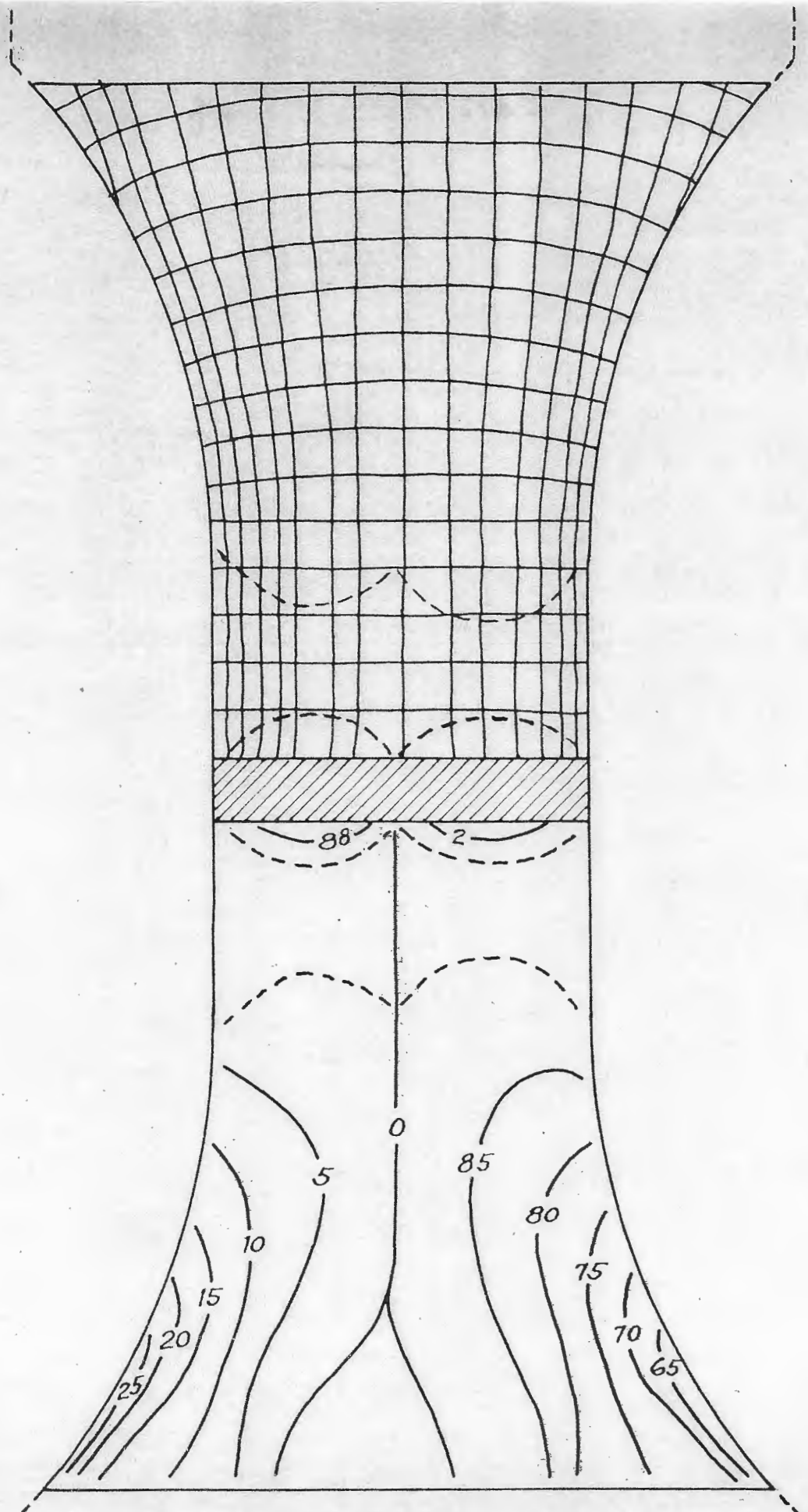

ISOSTATIC AND ISOCLINIC MAPS, MODEL F 4.8 R.

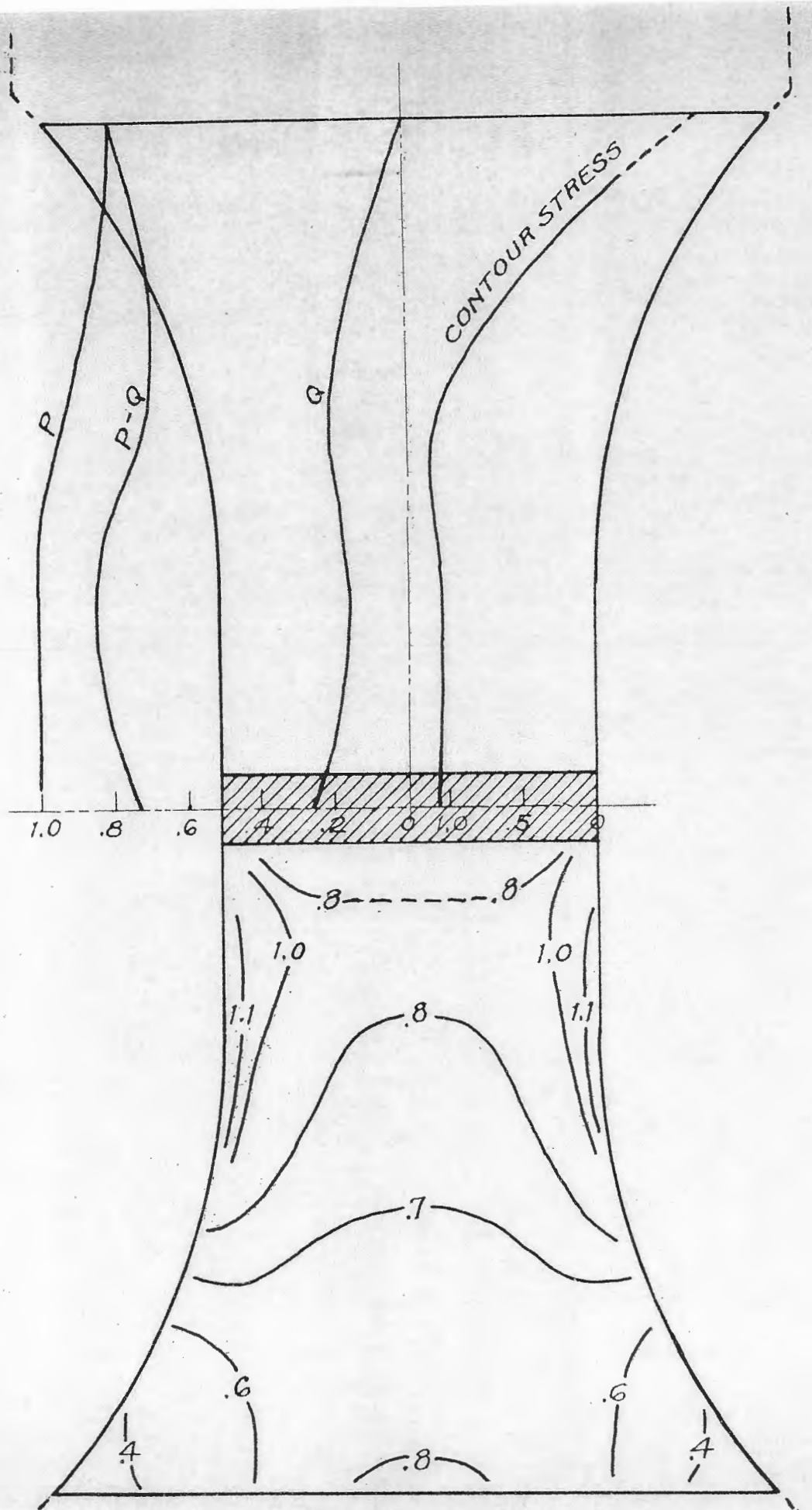

STRESS CURVES AND ISOCHROMATIC MAP, MODEL F 4.8 R.

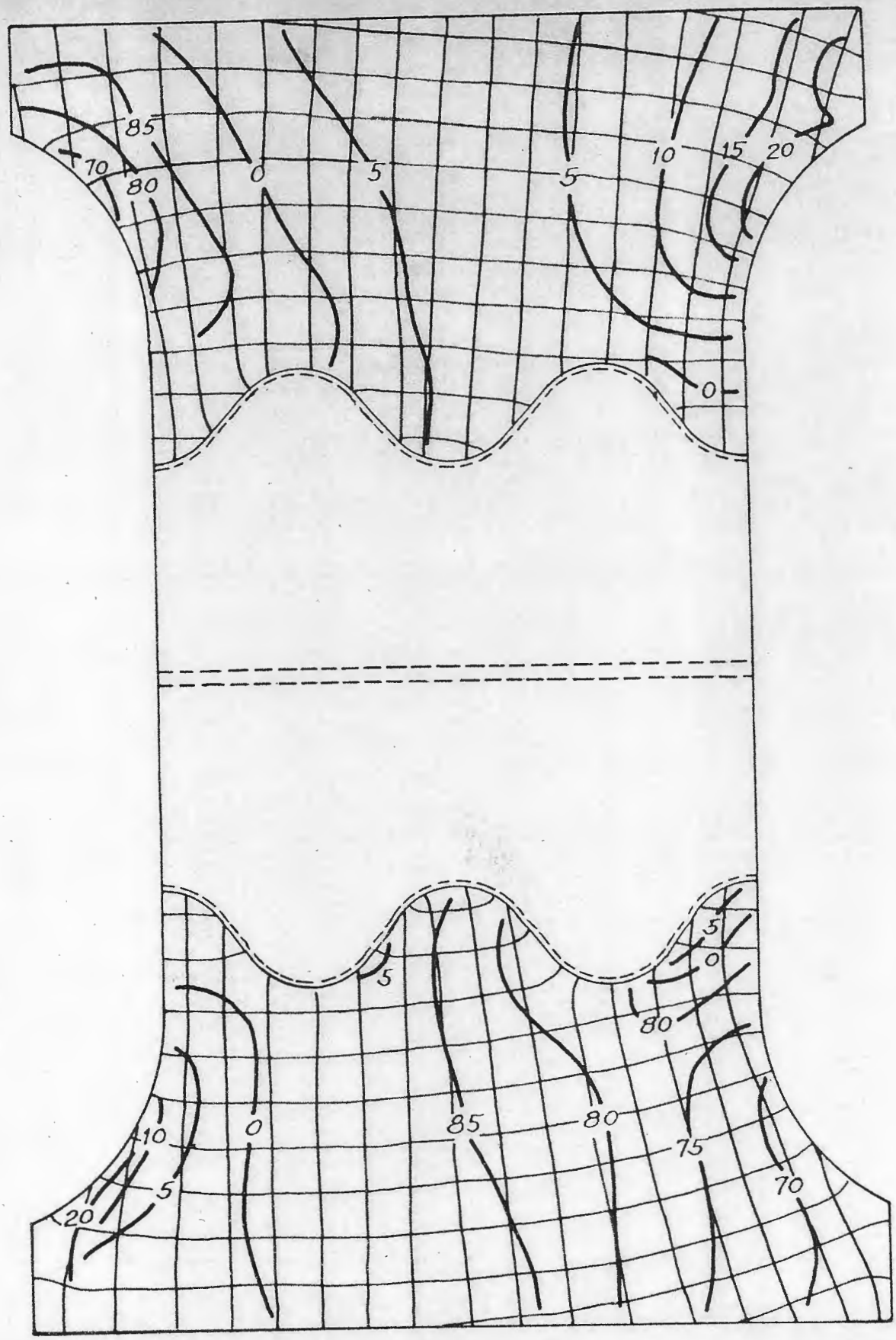

ISOCLINIC AND ISOSTATIC MAPS, MODEL B 1.7 R.

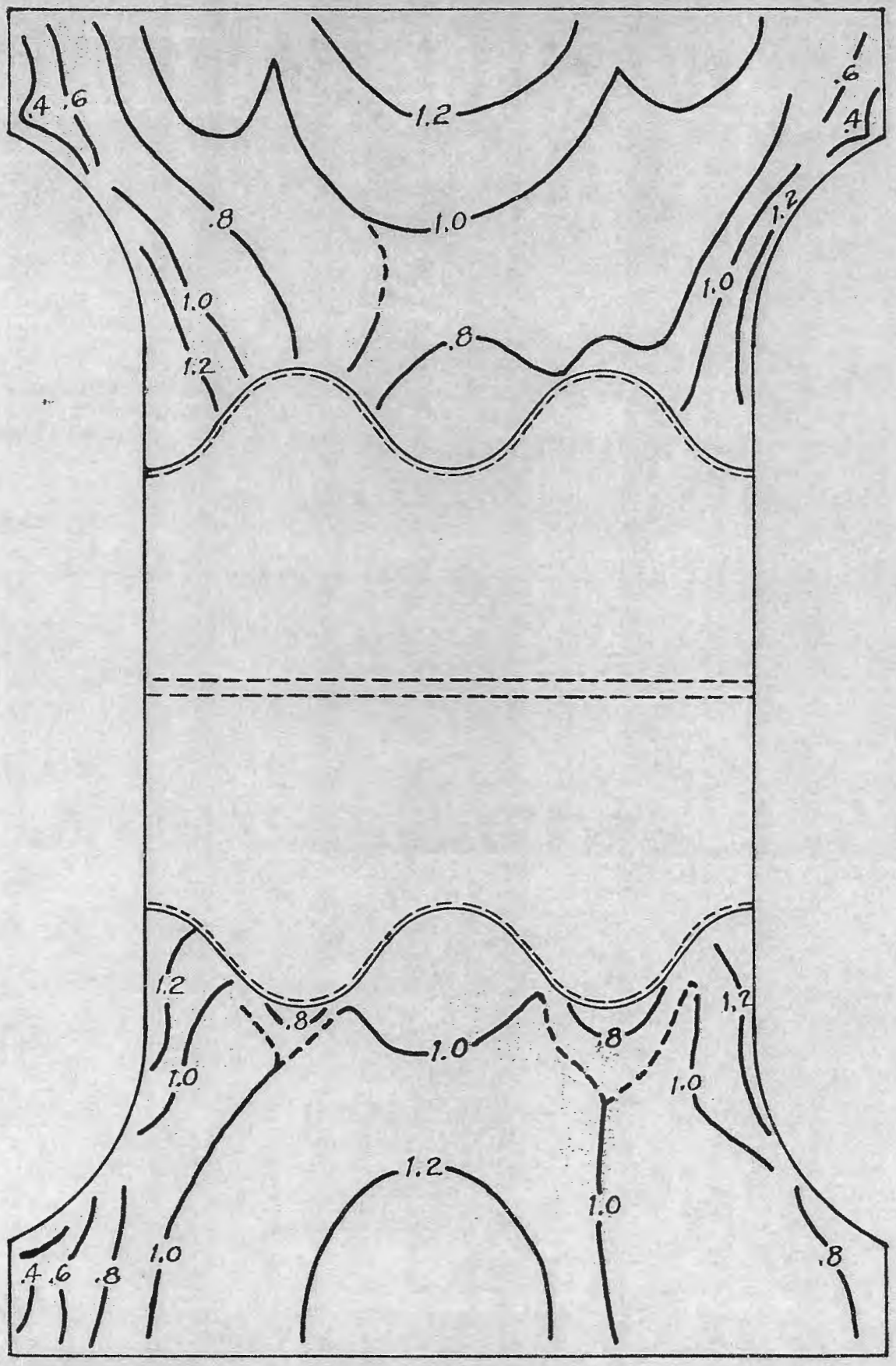

ISOCHROMATIC MAP, MODEL B 1.7 R.

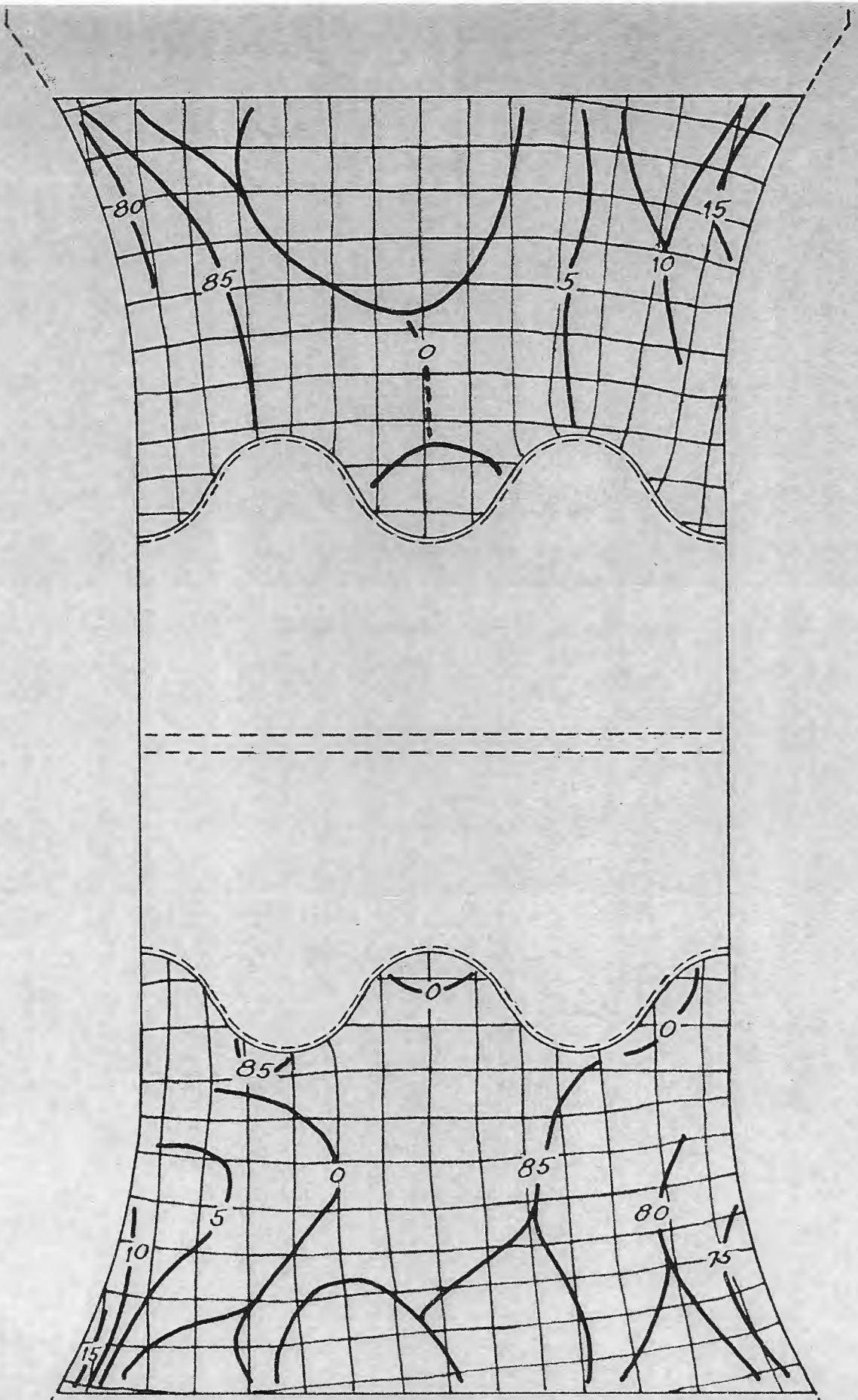

ISOCLINIC AND ISOSTATIC MAPS, MODEL B 4.8 R.

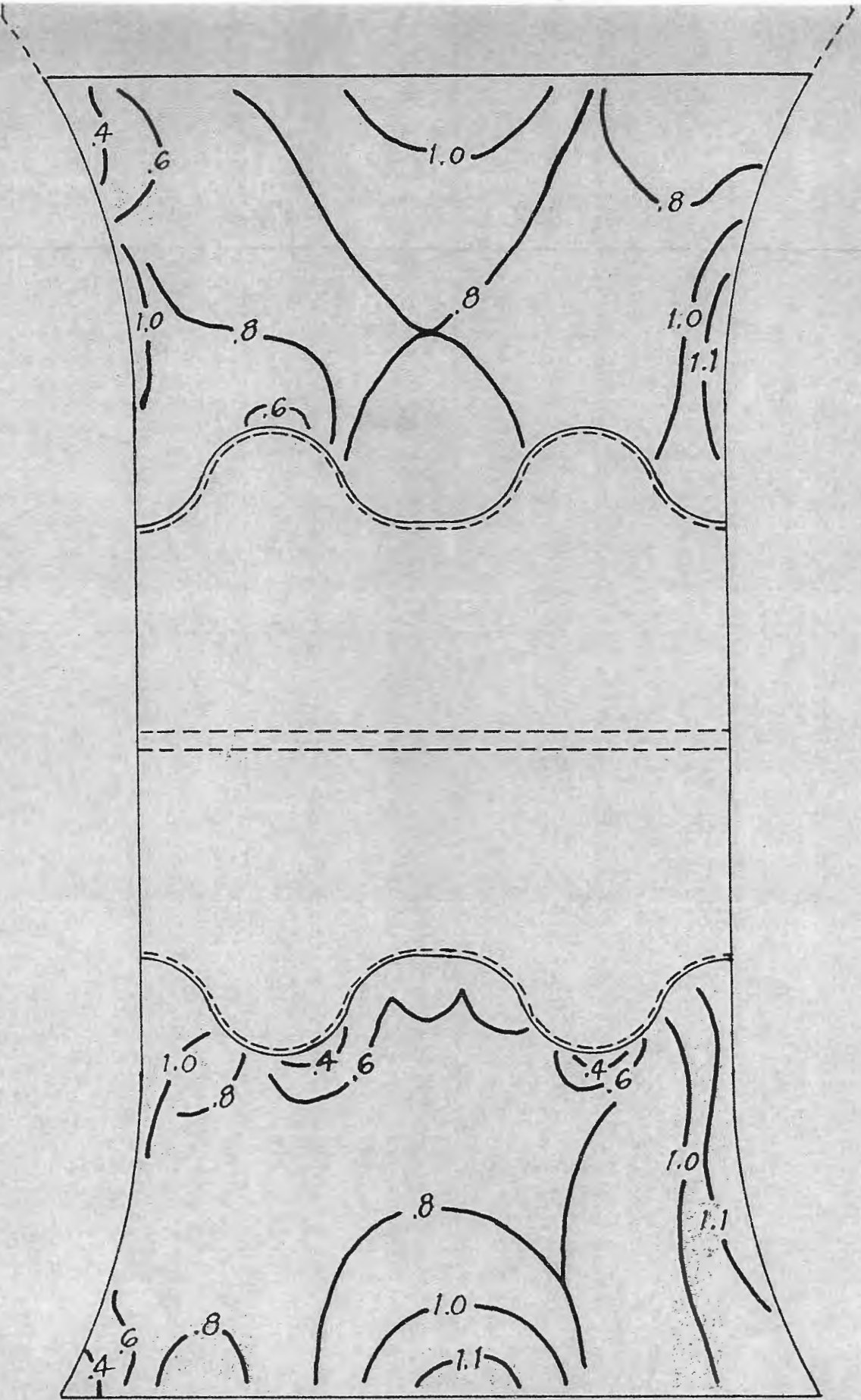

ISOCHROMATIC MAP, MODEL B 4.8 R.

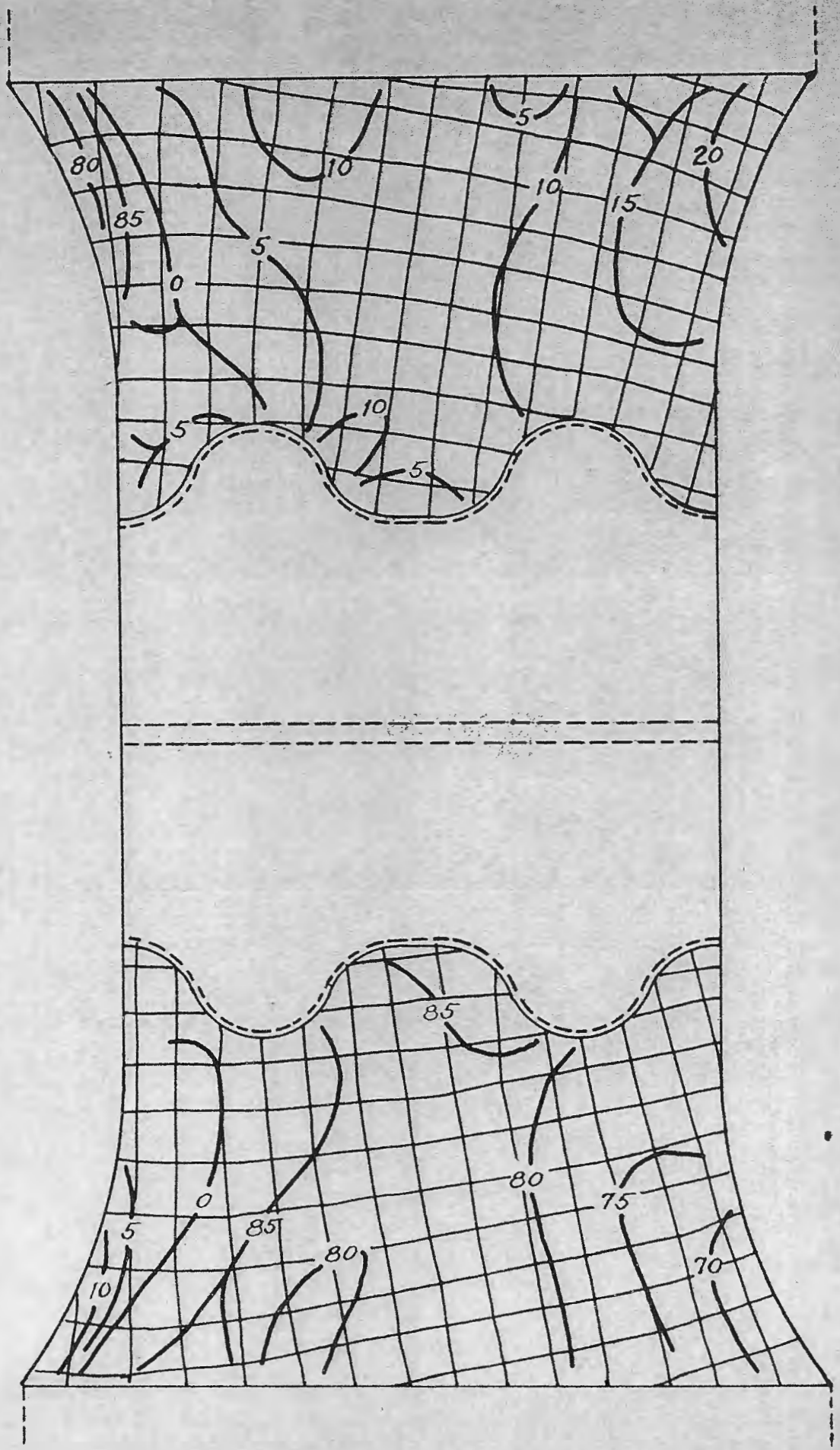

ISOCLINIC AND ISOSTATIC MAPS, MODEL C 4.8 R.

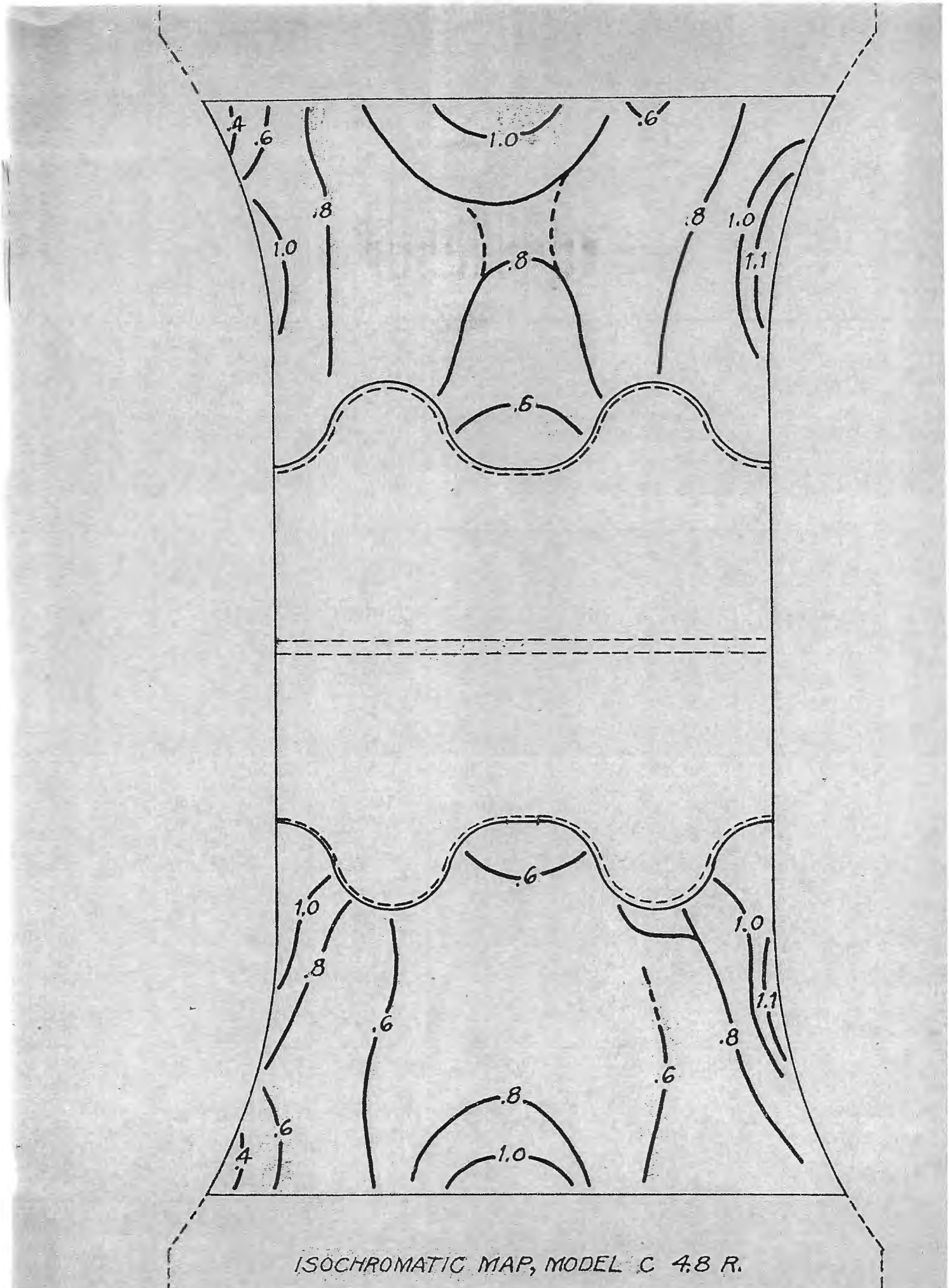

ISOCHROMATIC MAP, MODEL C 4.8 R.

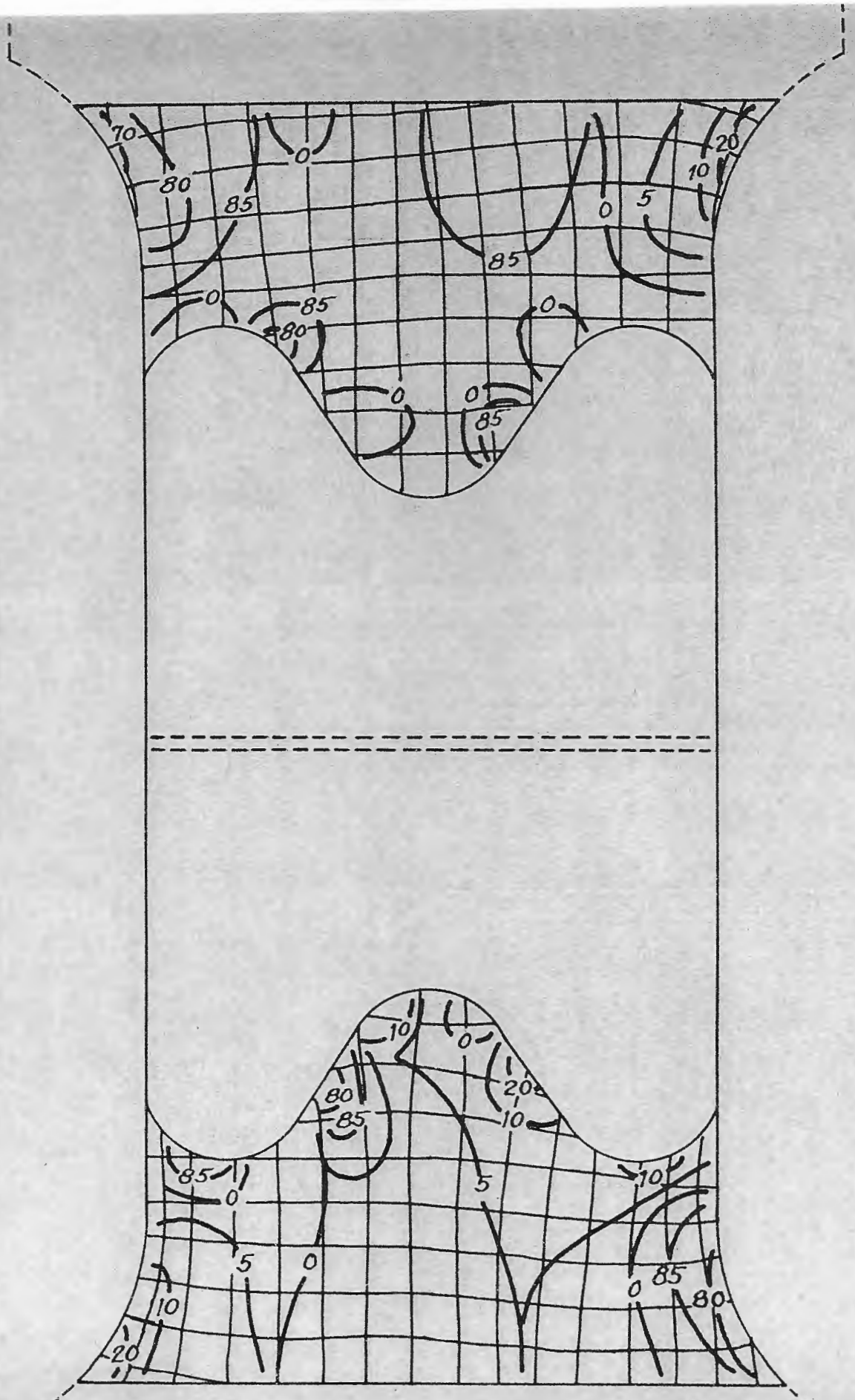

ISOCLINIC AND ISOSTATIC MAPS, MODEL D 1.8 R.

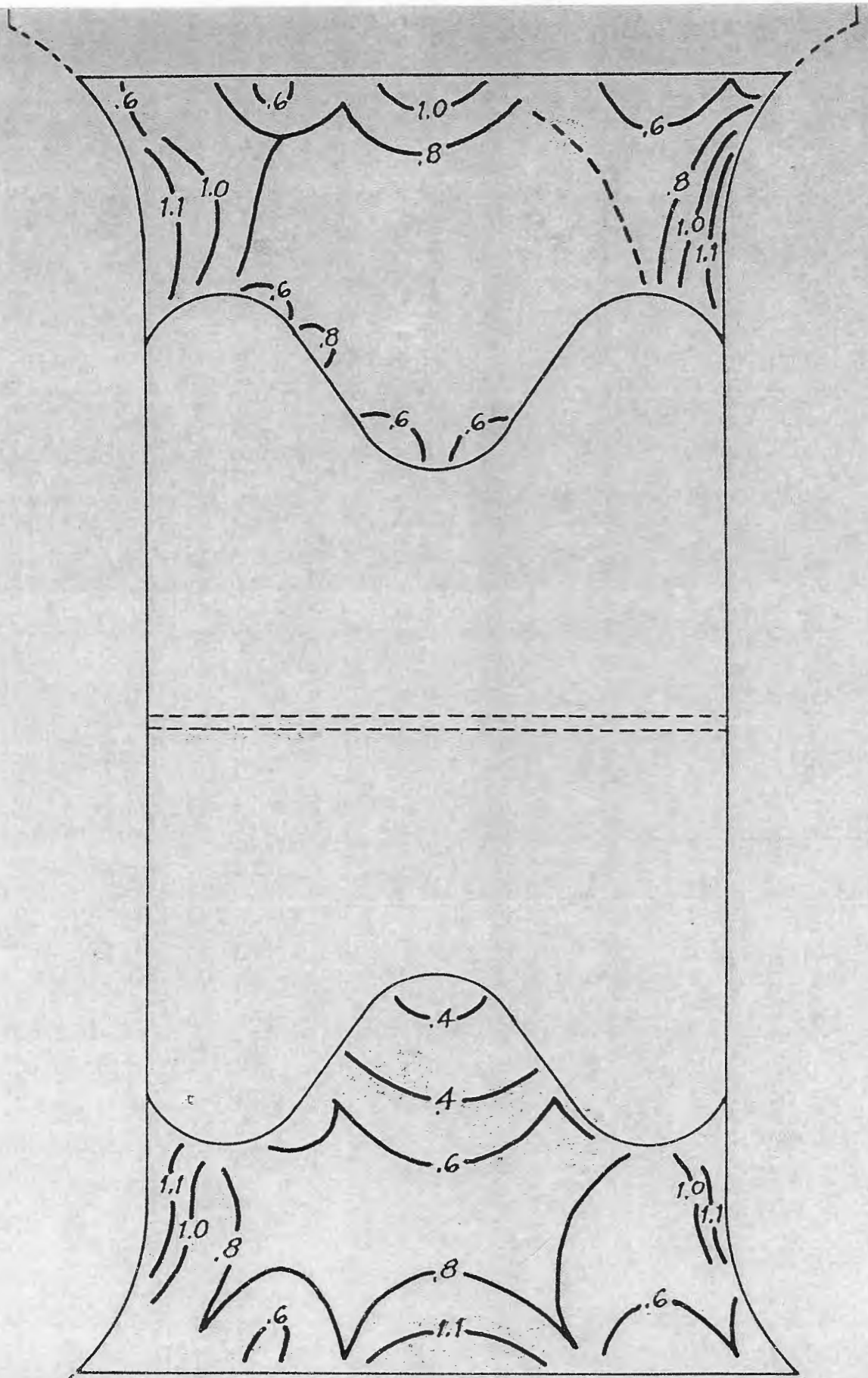

ISOCHROMATIC MAP, MODEL D 1.8 R.

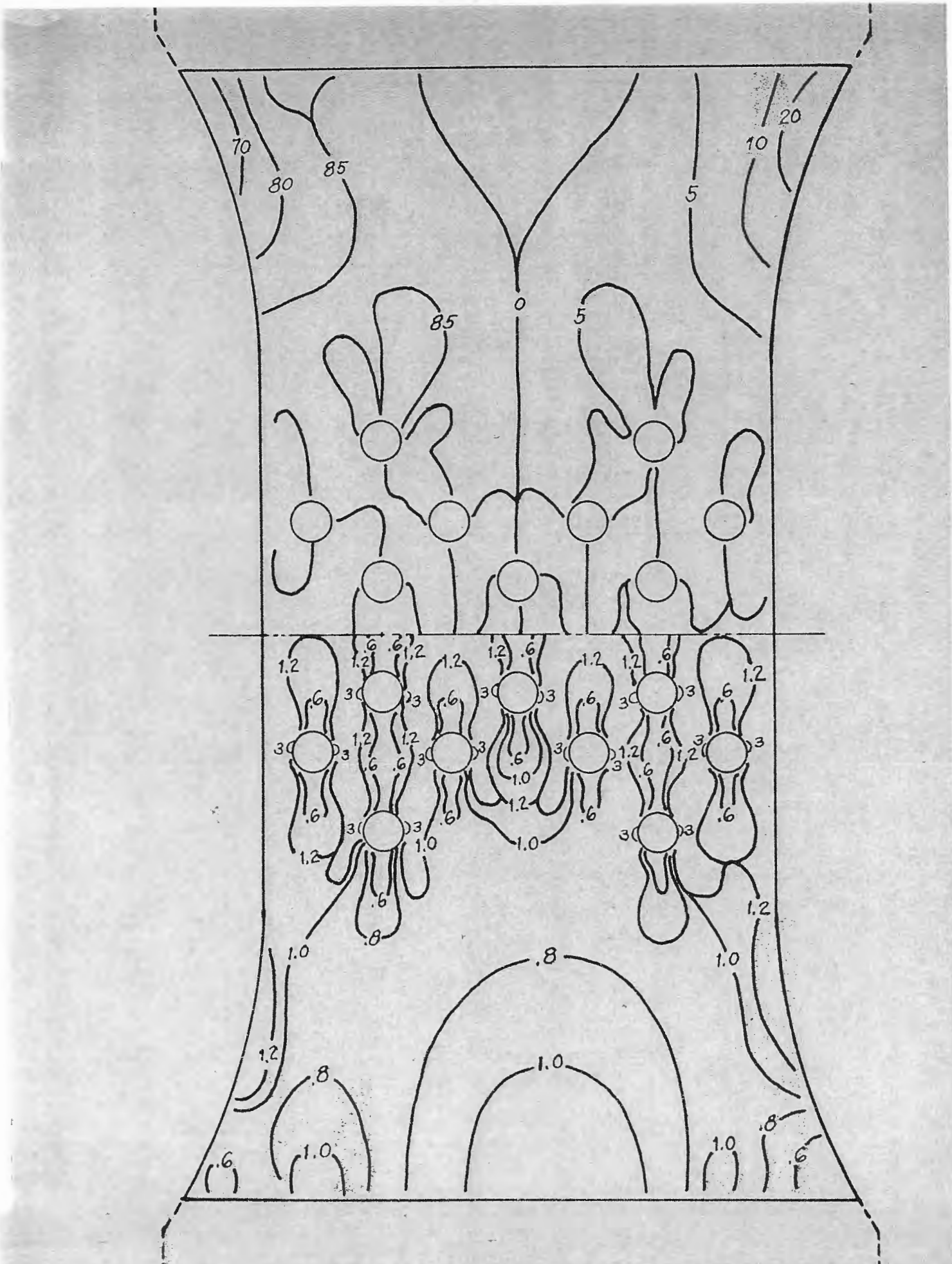

ISOCLINIC AND ISOCHROMATIC MAP, PLAIN MODEL.

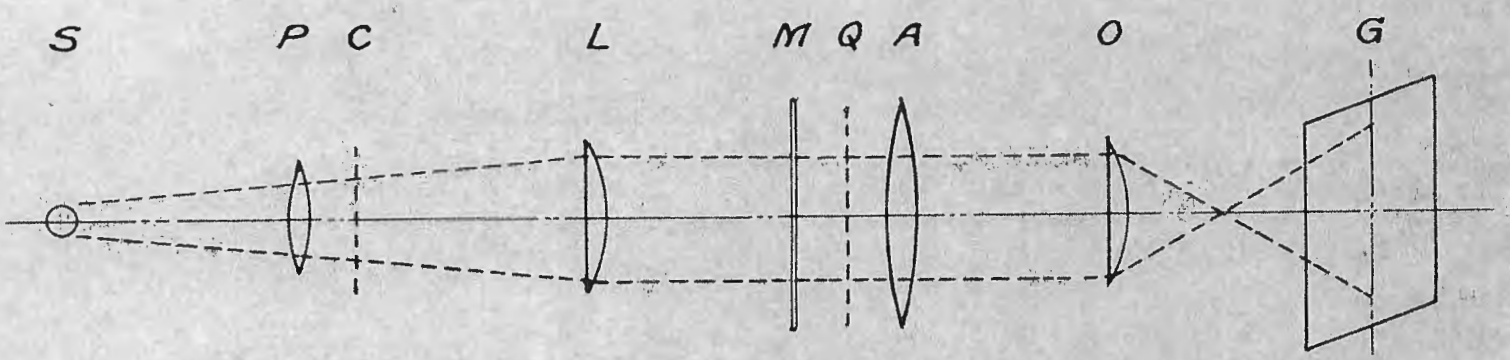

SCHEMATIC DIAGRAM OF OPTICAL ARRANGEMENT.

S - LIGHT SOURCE
P - POLARIZER
C - COMPENSATOR OR QUARTER WAVE PLATE
L - LENS
M - MODEL
Q - QUARTER WAVE PLATE
A - ANALYZER
O - OBJECTIVE
G - GROUND GLASS SCREEN.

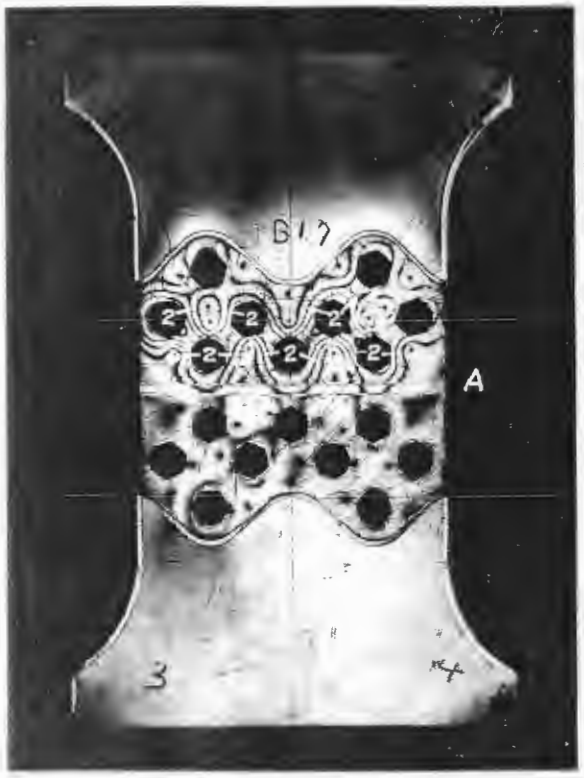

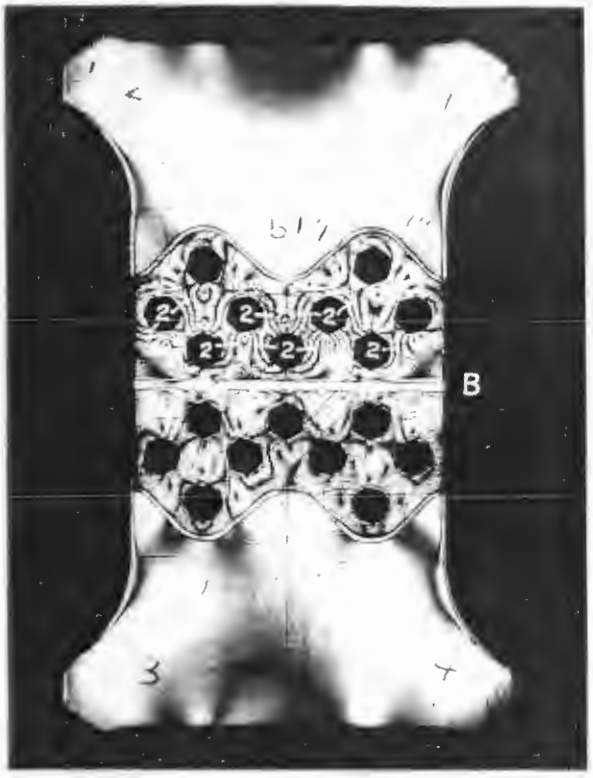

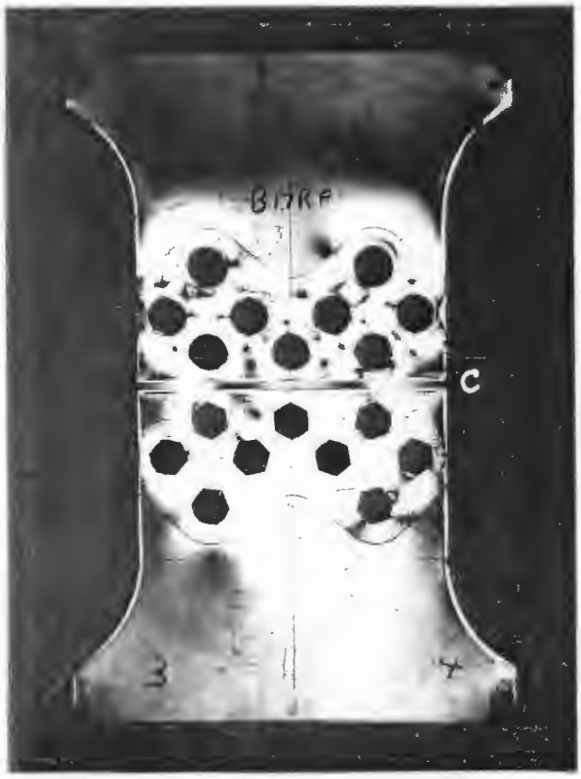

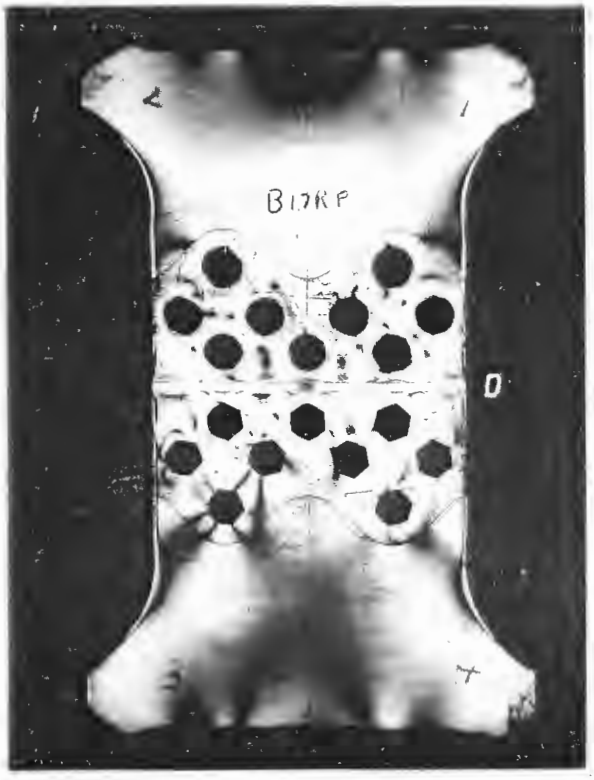

PLATE 23

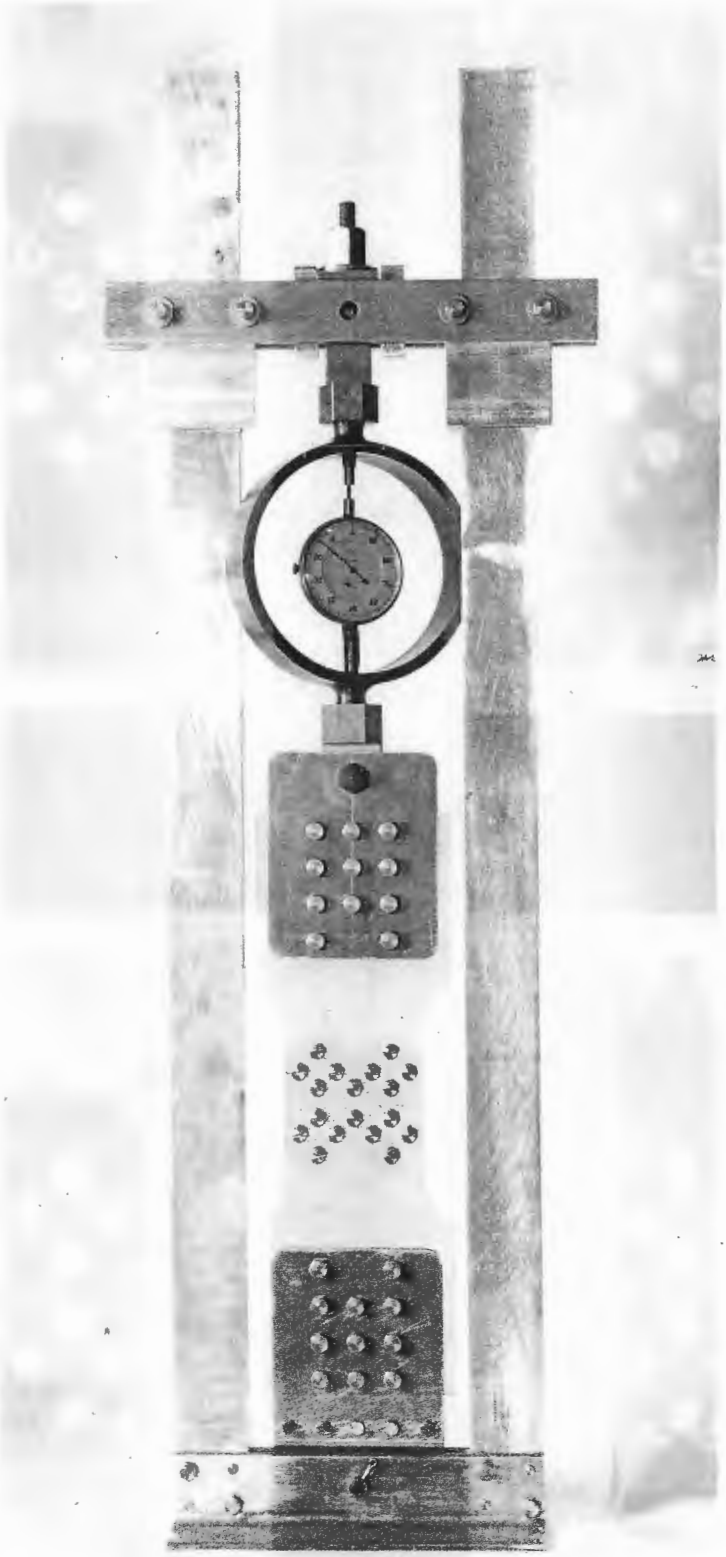

PLATE 24